# Chapter 6
# Targeted electrophysiological analysis of viscerofugal neurons in the myenteric plexus of guinea pig colon

# INTRODUCTION

Enteric viscerofugal neurons form the afferent pathway of reflex circuits between the gut and sympathetic prevertebral ganglia which regulate motility (Weems and Szurszewski, 1977) and secretion (Quinson and Furness, 2002). Mechanical distension of the gut activates these reflexes, and directly evokes viscerofugal neuron firing (Kuntz, 1940, Kuntz and Saccomanno, 1944, Hibberd et al., 2012c). However, viscerofugal neurons also receive prominent synaptic inputs via nicotinic receptors. This was shown by intracellular recordings from sympathetic prevertebral neurons, which receive synaptic inputs from viscerofugal neurons. During nicotinic blockade in the gut wall, decreases in both ongoing and distension-evoked synaptic activity were observed (Crowcroft et al., 1971b, Bywater, 1993). Subsequent intracellular recordings of viscerofugal neurons demonstrated directly that they indeed receive fast excitatory nicotinic inputs (Sharkey et al., 1998). Thus, viscerofugal neurons function in part as interneurons, and may comprise a pathway for transmitting output from enteric circuits to the sympathetic nervous system. However, the enteric pathways that converge upon viscerofugal neurons have not been functionally identified. Immunohistochemical evidence shows that cholinergic varicosities surrounding viscerofugal neurons appear to arise mainly from descending interneurons. Losses of synaptic inputs were observed immediately aboral, but not oral, to circumferential section of the myenteric plexus (Lomax et al., 2000). The major aim of the current study was to characterize the functional synaptic inputs to viscerofugal neurons in the myenteric plexus of isolated guinea-pig distal colon. This was performed by focal pharmacological activation of parts of myenteric ganglia, combined with intracellular recording of synaptic potentials in retrogradely labelled viscerofugal neurons.

## METHODS

*Dissection and DiI-labelling*

Adult guinea pigs, weighing 200-350g, were killed by stunning and exsanguination as approved by the Animal Welfare Committee of Flinders University. Segments of distal colon (10-20mm long, >20mm from the anus) and attached mesentery were removed and immediately placed into a Sylgard-lined petri dish (Dow Corning, Midland, MI) filled with filtered (polyethersulfone membrane, 0.22μm pores, Merck Millipore, Cork, Ireland) and oxygenated Krebs solution at room temperature. The Krebs solution contained (in mM concentrations): NaCl 118; KCl 4.7, $NaH_2PO_4.2H_2O$ 1; $NaHCO_3$ 25; $MgCl_2$.6H2O 1.2; D-Glucose 11; $CaCl_2.2H_2O$ 2.5; bubbled with 95%$O_2$ and 5%$CO_2$. Segments were cut open along the mesenteric border and pinned flat with the mucosa uppermost. The mucosa and submucosa were removed by sharp dissection. Extrinsic nerve trunks (5-10 trunks per preparation, 3-10mm long) were dissected free from surrounding mesentery. The fluorescent dye, 1,1'-didodecyl-3,3,3',3'-tetramethyl indocarbocyanine perchlorate (DiI; D383, Molecular Probes, Eugene, OR) was used for retrogradely labelling viscerofugal neurons. DiI was evaporated from ethanol solution onto small glass beads (212-300μm diameter; G-1277, Sigma, St. Louis, MO). A single glass bead was gently placed onto each dissected extrinsic nerve trunk and was confirmed to have remained on the nerve during and after organ culture.

*Organotypic culture*

Following repeated washes with filtered Krebs solution, preparations were re-pinned into sterilized petri dishes containing sterile culture medium (Dulbecco's modified

Eagle's [DME]/Han's F12, Sigma [1:1 ratio mix, supplemented with L-glutamine and 15 mM HEPES]; including 10% fetal bovine serum (Gibco, Life Technologies Corporation, USA), 100 IU/ml penicillin (Pen Strep, Gibco), 100 µg/ml streptomycin D (Pen Strep, Gibco), 10 µg/ml gentamycin (Gibco), 2.5 µg/ml amphotericin B (Sigma), and 1.8 mM $CaCl_2$. The preparations were incubated for 2-4 days in a humidified incubator (36°C, 5% $CO_2$ in air), and agitated on a rocking tray. Sterile culture medium was changed every 24 hours.

*Intracellular recording*

Preparations were pinned, using 50µm tungsten pins, circular muscle uppermost, into a Sylgard-lined recording chamber of 1ml volume (**figure 6.01**). Circular muscle was removed by sharp dissection, leaving a preparation of longitudinal muscle and myenteric plexus. The recording chamber was fixed onto the stage of an inverted microscope (IX71, Olympus Corporation, Japan) fitted with fluorescent optics. Krebs solution at 35°C was constantly superfused at a rate of 3 ml/min. Neurons were impaled using borosilicate glass capillary electrodes (1 mm OD, 0.58 mm ID; Harvard Apparatus) filled with 5% 5,6-carboxyfluorescein (Sigma; 21877) in 20 mM Tris buffer (pH 7.0) in 1 M KCl solution (Carbone et al., 2012). Electrode resistances ranged from 110 to 175MΩ. Membrane potential of viscerofugal neurons were recorded using an Axoclamp 2A amplifier (Axon Instruments), viewed on an oscilloscope (model VP-5220A, Matsushita), digitized at 10 kHz, and stored via an analog-to-digital interface (MacLab 8SP, ADInstruments, Sydney, Australia) using Chart 7 software (ADInstruments). Single pulse electrical stimuli (0.4-ms, 10-15V) were delivered focally to local internodal strands or ganglia via paired Pt-Ir wire stimulating electrodes, insulated to 1mm of the tips, placed 0.5mm circumferential to

the recording electrode. A Grass S48 stimulator and a Grass S1U5 stimulator isolation unit were used to generate the stimulus. The nicotinic receptor agonist, 1,1-dimethyl-4- phenylpiperazinium iodide (DMPP; 10μM in Krebs solution, mixed 1:10 with blue food dye, Rainbow Food Colours, Australia), was applied focally to the tissue through a glass micropipette (10–20μm tip; illustrated in **figure 6.01** and shown in a photomicrograph in **figures 6.23**). Agonists were delivered using nitrogen gas under 70-80kPa pressure via a solenoid-operated valve driven by short electrical pulses 20–50ms in duration. Visualization of the spatial field and trajectory of drug ejection was enabled by the dye; ejection of dye solution without DMPP was used as a control. Locations of the recording and stimulating electrodes, and all sites tested with DMPP were recorded on photomicrographs (Camedia, C3040ZOOM, Olympus Corporation, Japan).

*Targeted impalements*

DiI-filled neurons were visualized using narrow-band LEDs of the appropriate excitation wavelength and emission filters (Cool LED *p*E excitation system, Andover, UK). To avoid damaging DiI-filled neurons, exposure to green excitation wavelength photons was limited by using low power objectives (20x), reducing current to LEDs to a minimum required for visualization, and by using short exposure time (<1s). Microelectrode tips were vertically aligned with the centre of the cell body and advanced using the vertical drive of a micromanipulator.

*Immunohistochemistry*

Preparations were maximally stretched and fixed in modified Zamboni's fixative (2% formaldehyde, 0.2% saturated picric acid in 0.1M phosphate buffer, pH 7.0)

after recordings. Tissue was then cleared for 1 hour in bicarbonate buffered glycerol (0.5M sodium carbonate in 50%, 70% and 100% glycerol solutions, pH 8.6, 20 minutes each, in series). Cleared preparations were incubated with antisera to choline acetyltransferase (1:1,000) and nitric oxide synthase (1:1,000) at room temperature for two days. Preparations were rinsed three times in PBS and incubated with secondary antisera for 4 hours at room temperature. The primary antibodies were as follows: rabbit anti-choline acetyltransferase (cat. no. P3YEB generously provided by Dr. M. Schemann of Technische Universitat Muenchen,), and sheep anti-nitric oxide synthase (cat. no. K205, generously provided by Dr. P. Emson). Both antibodies have been characterized in western blots of guinea pig inferior mesenteric ganglia and pelvic ganglia (Olsson et al., 2006). Secondary antibodies were donkey anti-sheep immunoglobulin G conjugated to indodicarbocyanine: Cy5 (Jackson, cat. no. 713-175-147, dilution 1:100) and donkey anti-rabbit immunoglobulin G conjugated to indocarbocyanine: CY3 (Jackson, cat. no. 711-165-152; dilution 1:400).

*Microscopy, image analysis and processing*

Specimens were examined on an Olympus IX71 microscope (Olympus Corporation, Japan) equipped with epifluorescence and highly discriminating filters (Chroma Technology Co., Battledore, VT). Images were captured using a Roper scientific (Coolsnap) camera at 1392 x 1080 pixels, using AnalySIS Imager 5.0 (Olympus-SIS, Münster, Germany) and saved as TIFF files. Matched micrographs of immunohistochemically-labelled nerve structures were captured using a 40x objective water-immersion lens. All cell bodies classified as ChAT- or NOS-immunoreactive (IR) were present in micrographs where all pixels less than or equal

to three standard deviations above the mean value of background fluorescence had been removed. Biotinamide-labelled cell bodies were excluded from the sample when they were overlying another biotinamide-labelled cell body. Viscerofugal neuron cell bodies were mapped using a pair of linear scales (AG-11; Mitutoyo Corporation, Japan) attached to the X and Y axes of the microscope stage. Figures were generated from grayscale images adjusted for contrast and brightness in Adobe Photoshop (CS5, Adobe Systems Inc, San Jose, CA) and were cropped and resized to improve display of cell bodies.

*Drugs*

Stock solutions of $10^{-1}$M hexamethonium chloride (Sigma; H2138) and $10^{-1}$M DMPP in water (Sigma; D5891) were kept refrigerated and diluted to working concentrations in Krebs shortly before use.

*Statistical Analysis*

Statistical analysis was performed by Student's two-tailed t-test for paired or unpaired data and $X^2$ tests using IBM SPSS Statistics 20 for Microsoft Windows (release 20.0.0, IBM Corp., USA). Differences were considered significant if $p<0.05$. Results are expressed as mean ± standard deviation except where otherwise stated. The number of animals used in each set of experiments is indicated in lower case ''n''. NS denotes a non-significant finding ($p>0.05$).

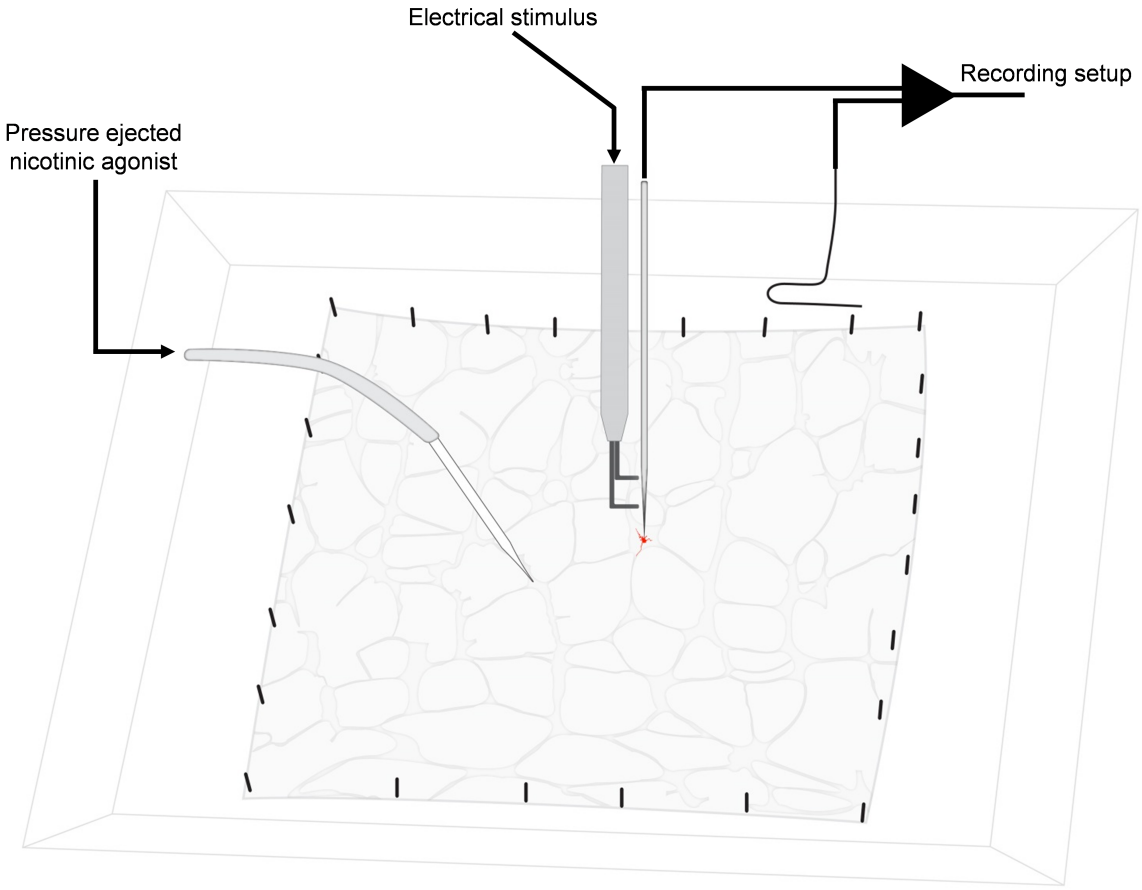


**Figure 6.01**

Schematic diagram of the experimental setup. This figure shows a longitudinal muscle/ myenteric plexus preparation that is pinned out in a small chamber with a recording electrode vertically aligned to a DiI-labelled viscerofugal neuron (shown in red). A stimulating electrode is positioned on an internodal strand projecting circumferentially to the ganglion that contained the viscerofugal nerve cell body. The tip of glass micropipette containing nicotinic receptor agonist (DMPP) was positioned close to surface of the tissue via a stage-mounted micromanipulator (not shown). The pipette tip was allowed a small clearance above the tissue surface to allow free movements around the chamber without contacting the preparation, which can dislodge impalements.

*DiI-tracing of viscerofugal neurons*

Viscerofugal neurons were retrogradely labelled from mesenteric nerve trunks with DiI, revealing their cell bodies (20 preparations, n=14, **figure 6.02** and **6.03**). The cell bodies of viscerofugal neurons were distributed close to the mesenteric border as described previously (Furness et al., 1990c). More than 75% of DiI-labelled nerve cell bodies were located within 1.5mm of the mesenteric border. The distribution of 401 DiI-labelled viscerofugal neurons from a sample of 10 preparations, including neurons which were impaled, is shown in **figure 6.04**. On average, there were 30 ± 15 DiI-labelled cell bodies per preparation (n=10). As is characteristic of DiI-tracing in live preparations (Brookes, 2001b), labelling appeared punctate in nerve cell bodies. The densest labelling occurred close to, but not within, the nucleus (this can be seen in **figure 6.03**).

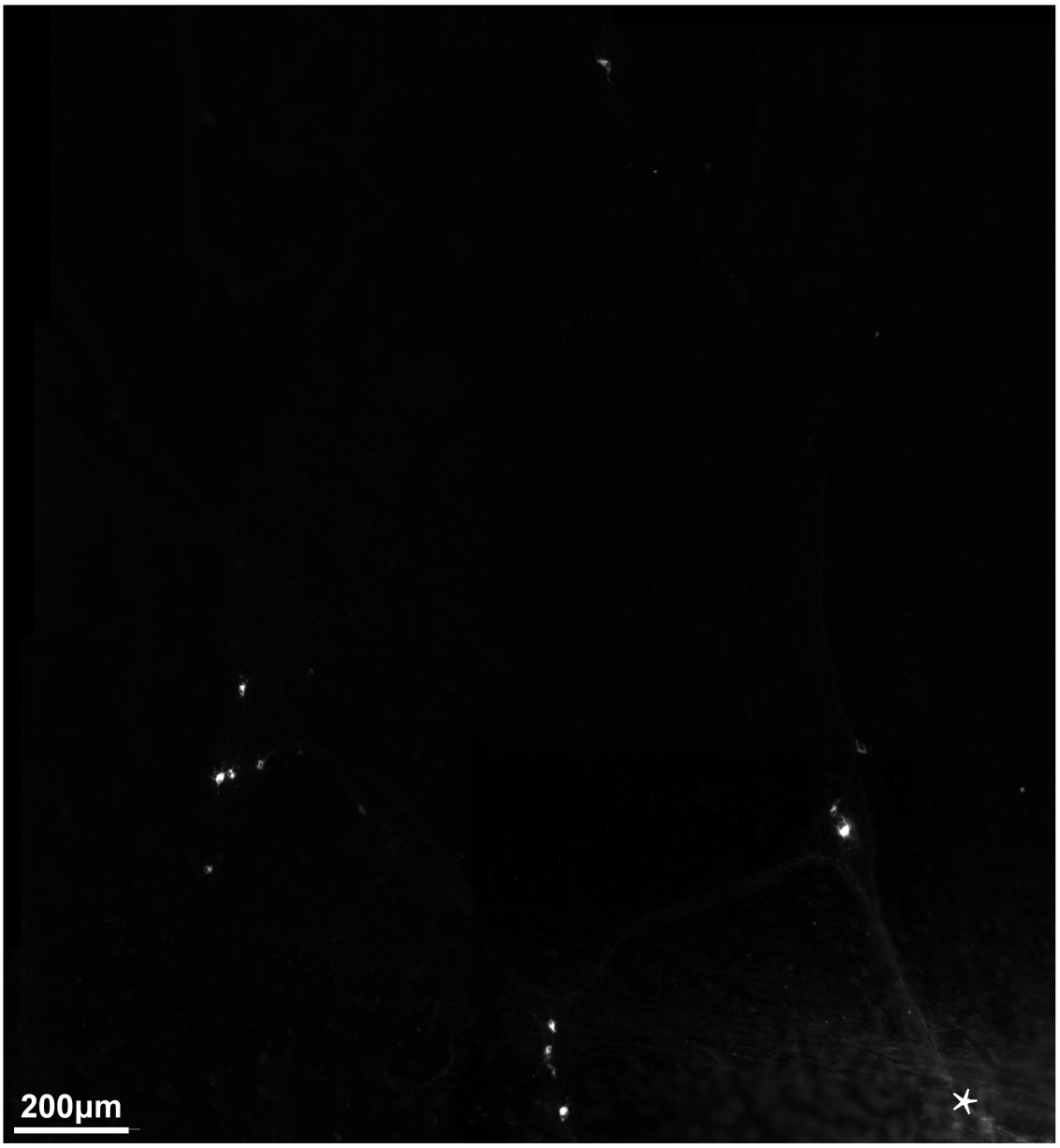


**Figure 6.02**

Low power photomontage of viscerofugal nerve cell bodies labelled from a colonic nerve trunk. Note 3 clusters of 3-5 viscerofugal nerve cell bodies. Although DiI more faintly reveals nerve axons, these viscerofugal neurons may be seen branching off the colonic nerve trunk from which their axons were labelled (marked with an asterisk). Overall, the appearance of DiI was strong in viscerofugal nerve cell bodies in comparison to their axons.

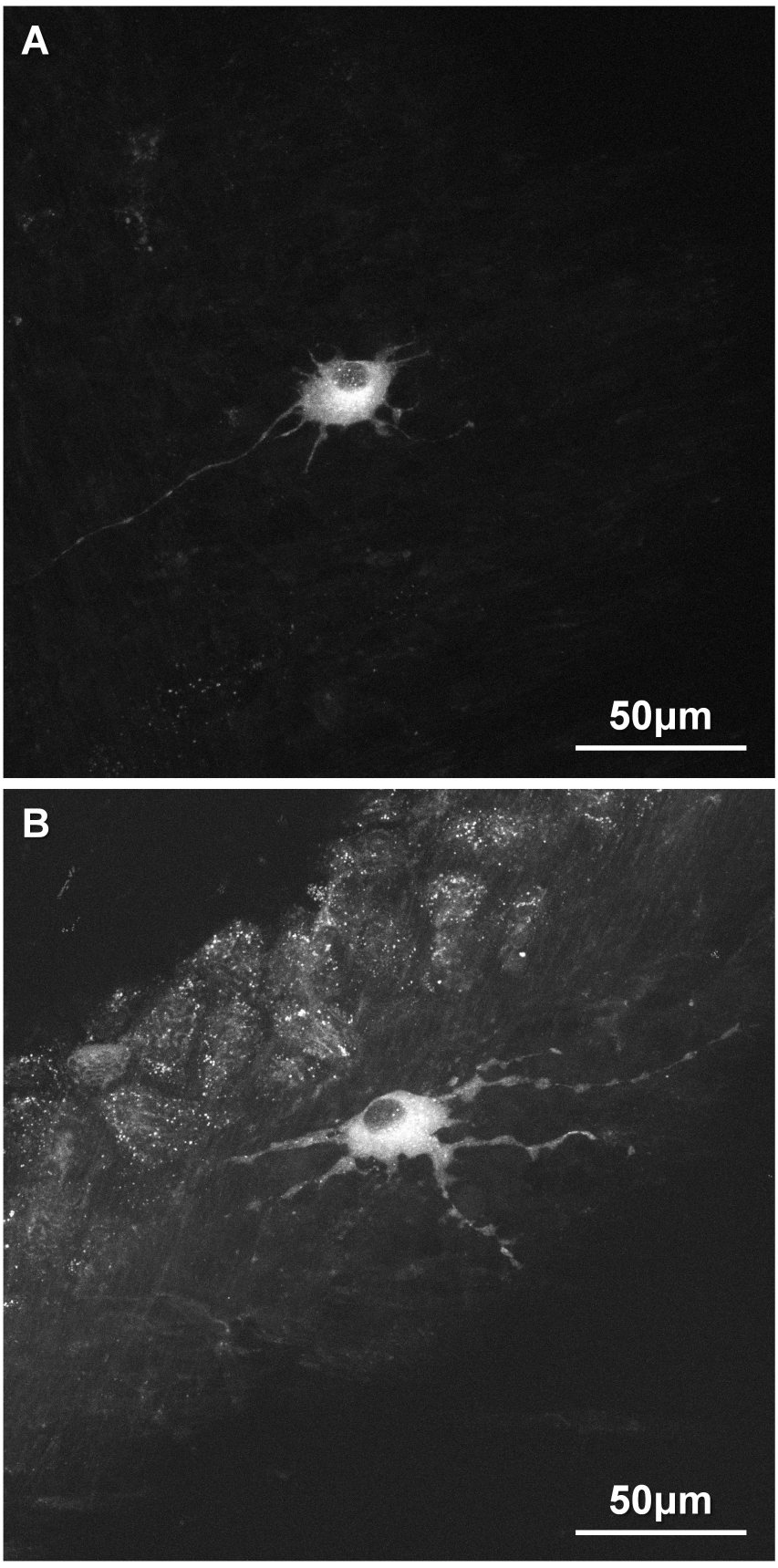


**Figure 6.03**

Confocal micrographs (maximum projection) of DiI-labelled viscerofugal nerve cell bodies. Shown in **A** is a viscerofugal neuron that has a small ovoid-shaped cell body from which several short dendrites and a single axon project. The viscerofugal neuron in **B** has an ovoid-shaped cell body with longer and thicker lamellar dendritic processes than the viscerofugal neuron in **A**.

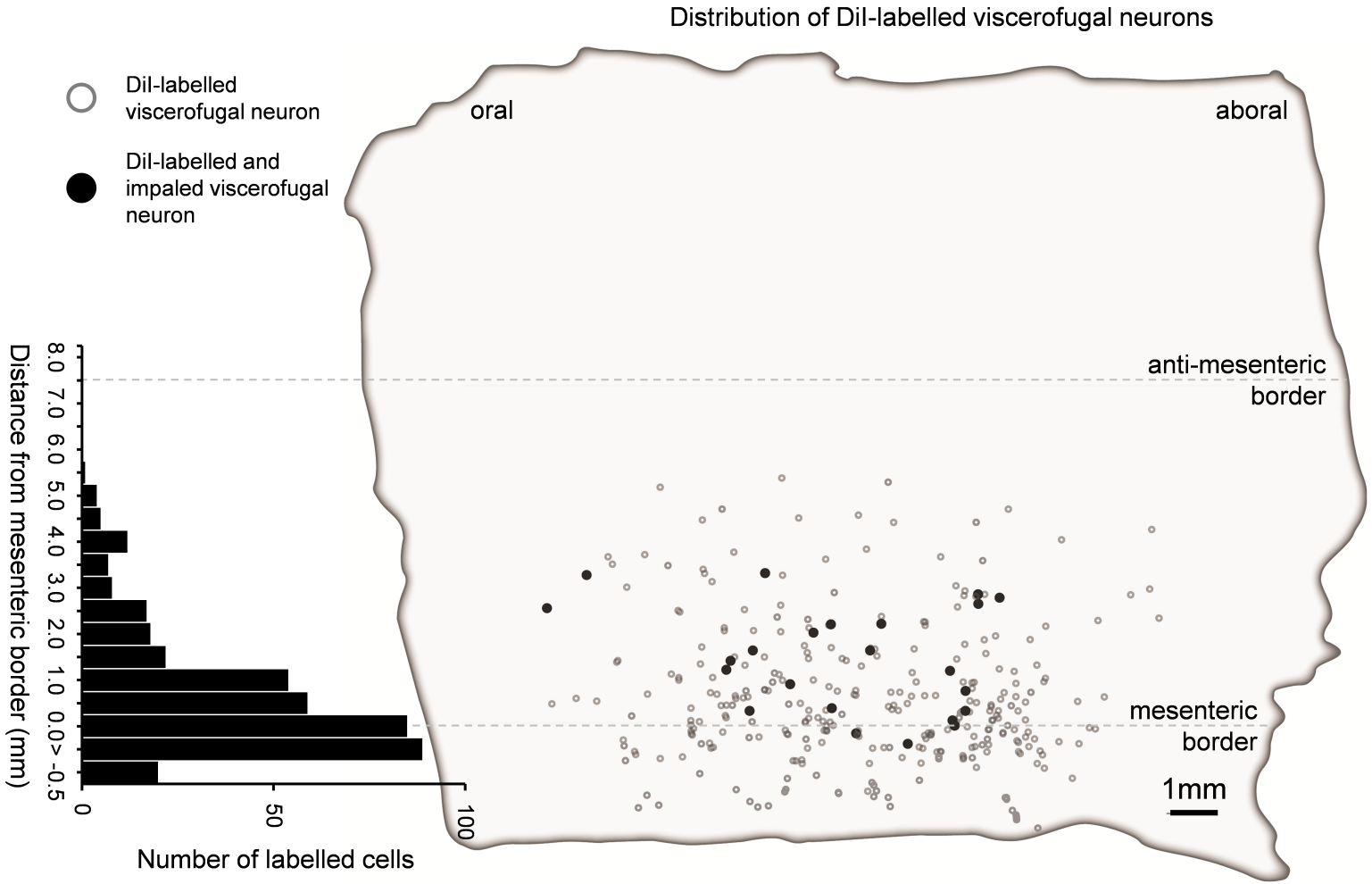


**Figure 6.04**

Composite map showing the distribution of DiI-labelled viscerofugal neuron cell bodies in 10 preparations of guinea pig distal colon. Here, the open grey circles indicate DiI-labelled viscerofugal nerve cell bodies. Shown in black circles are viscerofugal nerve cell bodies that were retrogradely labelled with DiI and impaled with microelectrodes. This figure shows 401 DiI-labelled viscerofugal neurons; impalements were made from 23 of these neurons. Note the circumferential distribution of viscerofugal neurons on the frequency histogram (adjacent the map). There was a high density of viscerofugal neurons close to the mesenteric border.

*Carboxyfluorescein-labelling*

Carboxyfluorescein dye was evident within DiI-labelled neurons after successful impalements. The cytoplasmic labelling of carboxyfluorescein revealed more detail in the morphology of cell bodies, dendrites and axons than the punctate DiI labelling (39 cells, **figures 6.05**, **6.06**, and **6.07**). Most dye-filled viscerofugal neurons either had small smooth cell bodies with a few or no dendrites (simple morphology, 12 cells, n=8), or had medium cell bodies with lamellar dendrites (Dogiel type I, 26 cells, n=12). Thirty-eight of 39 impaled viscerofugal neurons had single axons (**figure 6.06** and **6.07**); one viscerofugal neuron had multiple bifurcating axons and filamentous dendrites (**figure 6.08**), characteristic of dendritic Dogiel type II morphology described in colonic neurons (Lomax et al., 1999). In aggregated neuronal tracing studies, such multipolar viscerofugal neurons have been observed occasionally, but account for fewer than 1% of viscerofugal neurons. Additional examples of multipolar viscerofugal neurons are shown in **figure 6.09**.

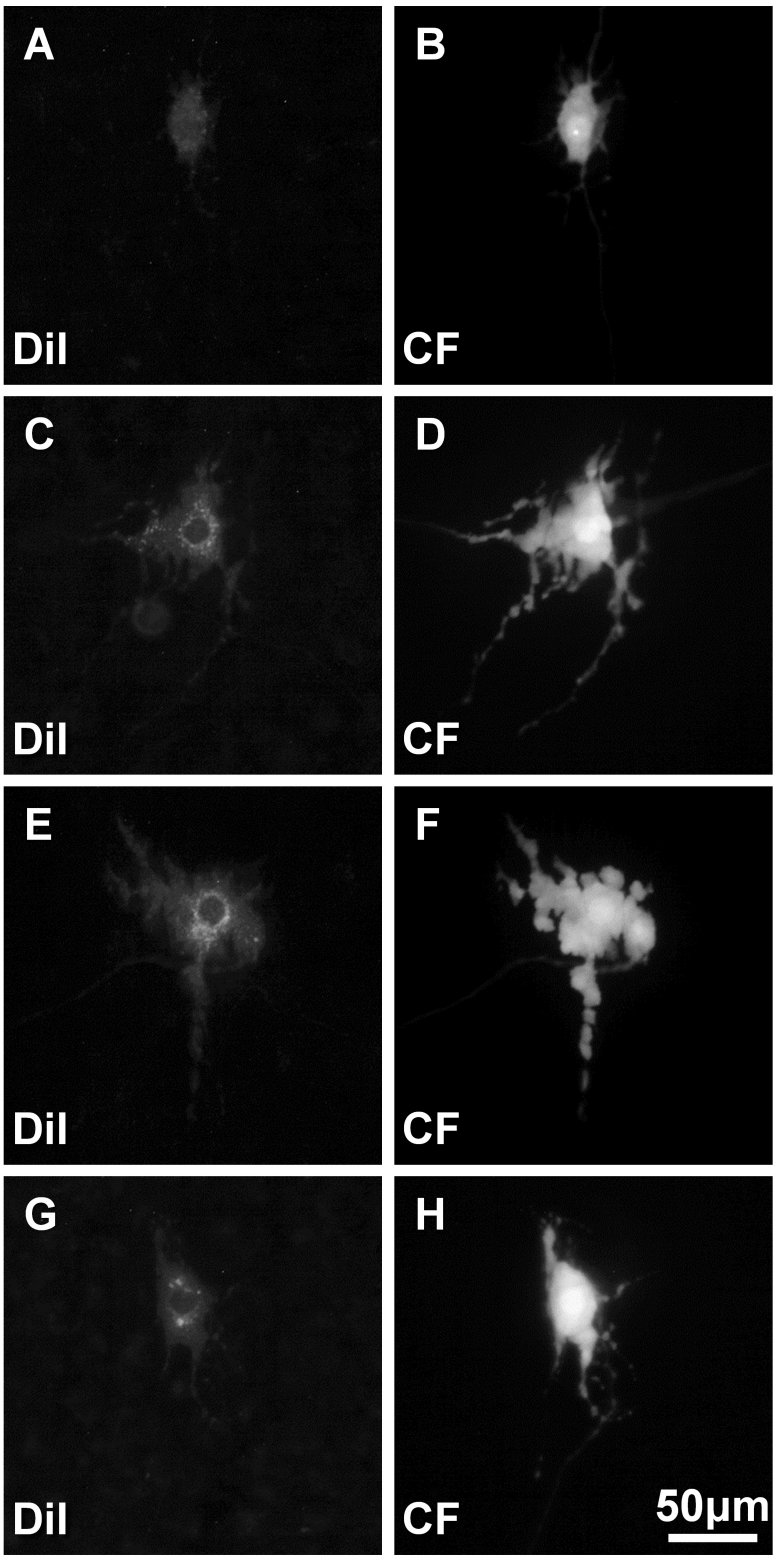


**Figure 6.05**

Simultaneous localisation of DiI and carboxyfluorescein in viscerofugal nerve cell bodies. Shown in **A-H** are matched micrographs of DiI and carboxyfluorescein (CF) in viscerofugal nerve cell bodies. These were taken in live preparations immediately after impalements, revealing that the targeted DiI-labelled viscerofugal neuron had been successfully recorded. The DiI-labelling was a punctate in appearance and concentrated around the cell nuclei. Carboxyfluorescein dye-filling was cytoplasmic in appearance and revealed in more detail the morphological characteristics of nerve cell bodies and dendrites.

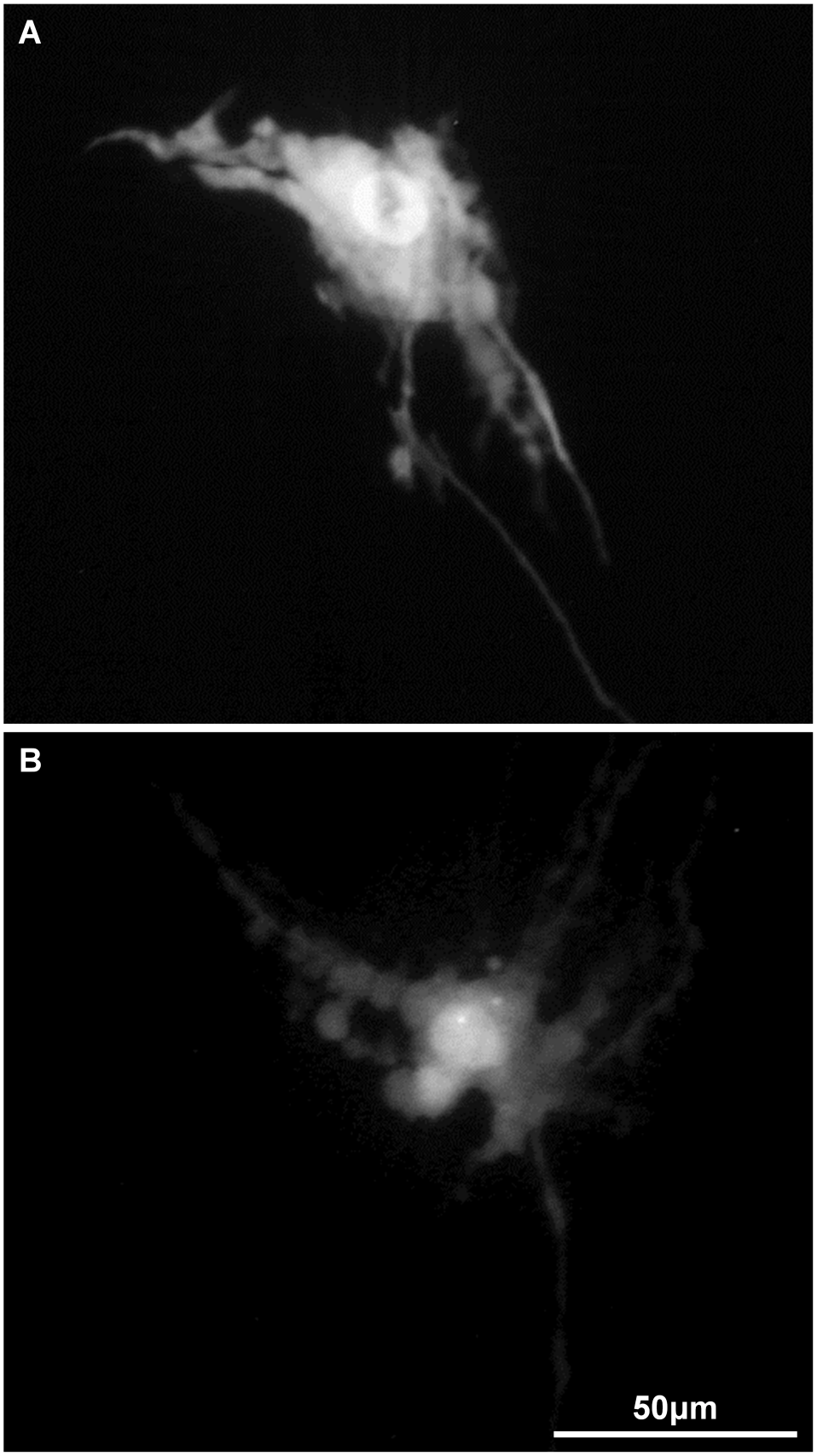


**Figure 6.06**

Lamellar viscerofugal neurons. Shown in **A** and **B** are viscerofugal neurons filled with carboxyfluorescein. These viscerofugal neurons had large nerve cell bodies, a single axon, and expansive lamellar dendrites.

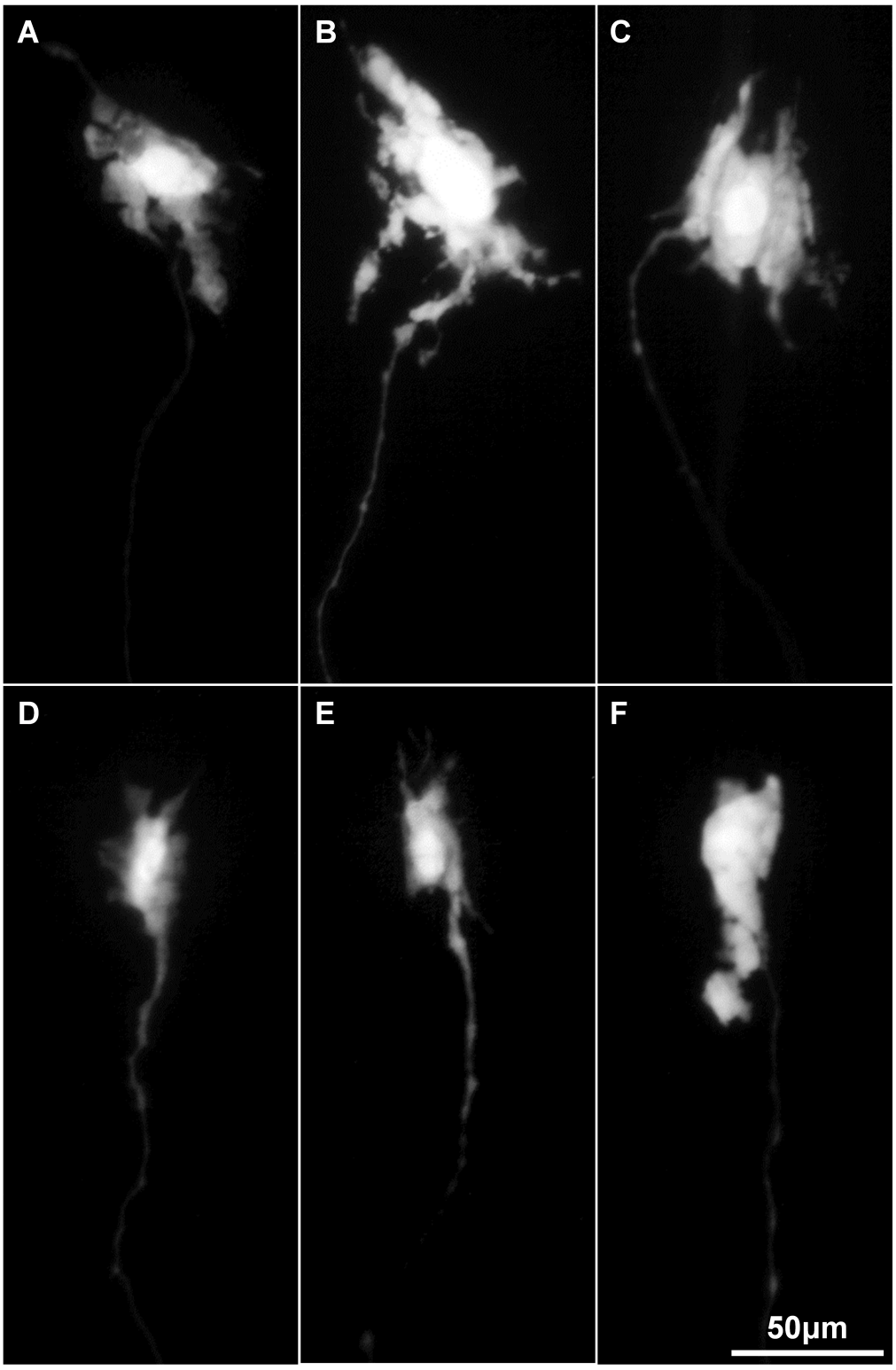


**Figure 6.07**

Carboxyfluorescein-labelled viscerofugal neurons. Micrographs **A**-**C** show neurons with large, irregularly shaped cell bodies and short lamellar dendrites. Micrographs **D**-**F** show viscerofugal neurons that have smaller, ovoid-shaped cell bodies, also with short lamellar dendrites. All viscerofugal neurons shown have a single axon.

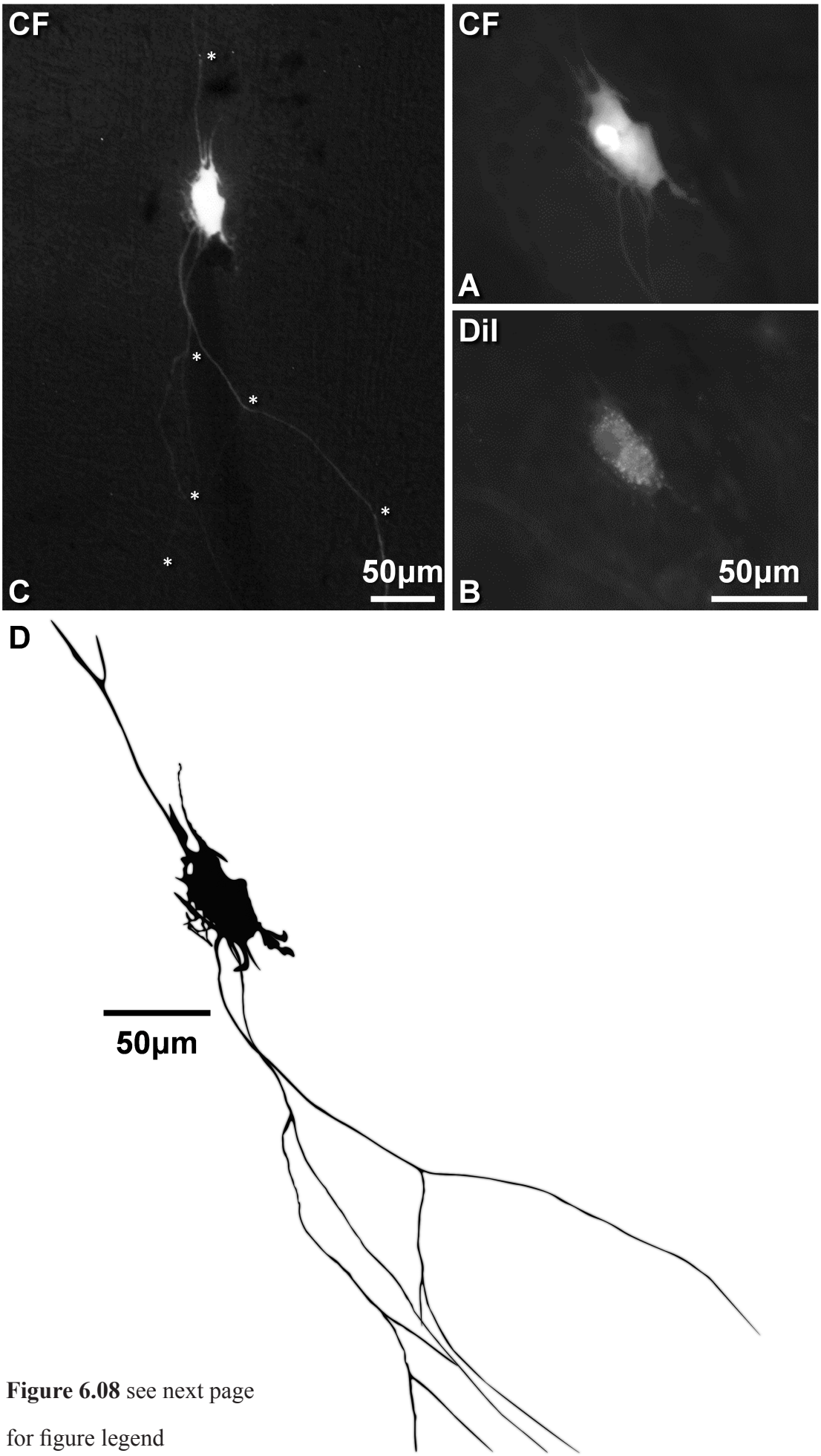


**Figure 6.08** see next page for figure legend

**Figure 6.08**

A multipolar viscerofugal neuron with dendritic Dogiel type II morphology. **A** and **B** show the simultaneous localisation of carboxyfluorescein and DiI in the viscerofugal nerve cell body. Shown in **C** is a lower power micrograph that was taken in the live preparation immediately after impalement. Note that several axonal processes can be seen emerging from the cell body. These axons can be seen bifurcating at points along each of the axons (marked with asterisks). Shown in **D** is a trace of the same neuron after fixation, revealing cell morphology more clearly. Note that some fading of carboxyfluorescein had taken place after fixation. In some cases this precluded discrimination of portions of the axons that are evident in the micrograph of the live preparation (**C**).

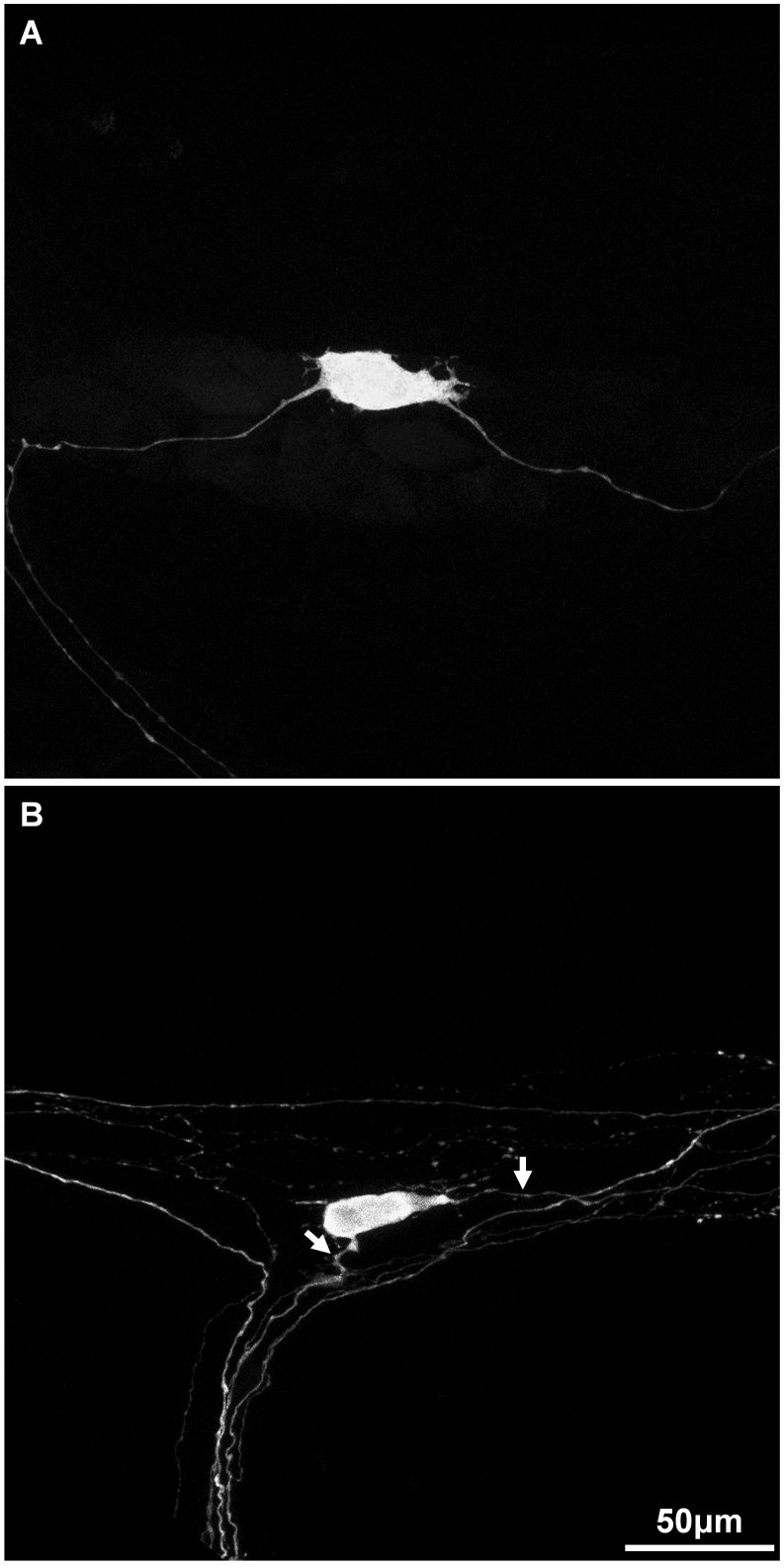


**Figure 6.09**

Confocal micrographs of multipolar viscerofugal neurons labelled with biotinamide. Multipolar viscerofugal neurons have been occasionally identified. Shown in **A** and **B** are examples of multipolar viscerofugal nerve cell bodies: the only examples among several hundred uniaxonal viscerofugal neurons that have been observed in accumulated neuronal tracing studies of extrinsic nerves to the gut. In **A** and **B**, the viscerofugal nerve cell bodies have two axons. Each axon in **B** is marked with an arrow.

*Immunohistochemistry*

Thirty-eight of 39 viscerofugal neurons were processed for immunohistochemistry after recordings; 1 cell was sacrificed in a pilot experiment. All eleven recorded viscerofugal neurons in 4 preparations that were incubated with ChAT antisera contained ChAT immunoreactivity (11/11 cells, n=4, **figure 6.11**). Of a total of 120 viscerofugal neurons that were labelled with DiI in the same 4 preparations, 105 contained ChAT immunoreactivity (87.5%). Twenty-seven electrophysiologically recorded viscerofugal neurons were tested for NOS immunoreactivity; 20/27 cells contained NOS immunoreactivity (74%, n=10, **figure 6.10** and **6.11**). Of 254 DiI-labelled viscerofugal neurons that were not used for electrophysiology, 105 (41.3%, n=10) contained NOS immunoreactivity. This suggests that intracellular recordings were biased in favour of NOS-immunoreactive neurons ($X^2$=10.59, df=1, $p<0.001$, standardized residual = + 2.3), probably because of their greater size. Nerve cell bodies of NOS immunoreactive viscerofugal neurons were significantly larger than viscerofugal neurons lacking NOS (994 ± 410μm$^2$ vs. 566 ± 212μm$^2$, respectively, $p<0.05$, t-test).

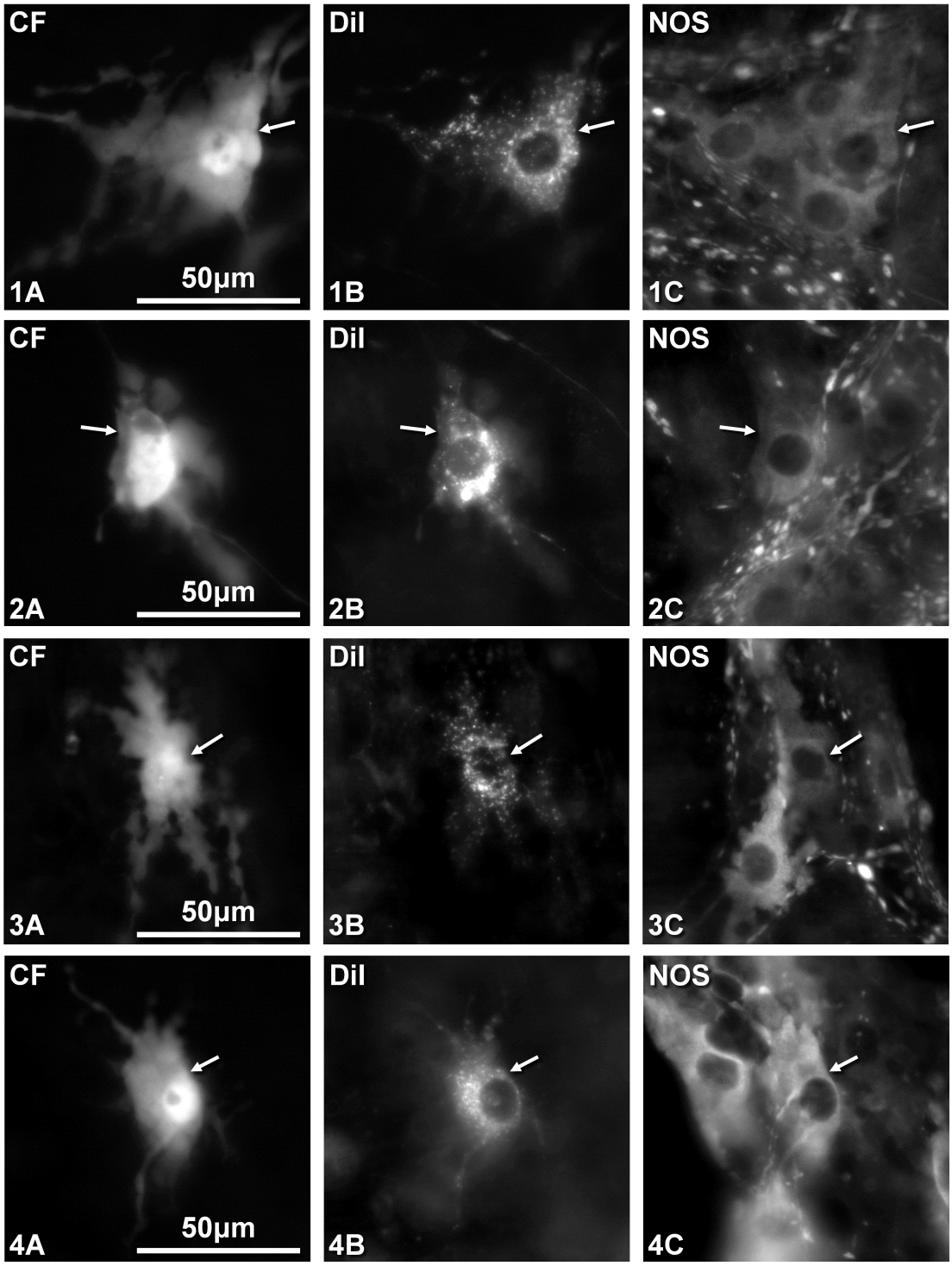


**Figure 6.10**

Micrographs of viscerofugal neuron cell bodies that contain immunoreactivity for nitric oxide synthase. These micrographs are matched horizontally, showing carboxyfluorescein (**1A-4A**), DiI (**1B-4B**) and immunoreactivity for nitric oxide synthase (**1C-4C**). Note the cytoplasmic labelling of carboxyfluorescein and punctate labelling of DiI. Immunoreactivity for nitric oxide synthase can be seen surrounding the nucleus in the nerve cell body and within cell processes in all viscerofugal neurons.

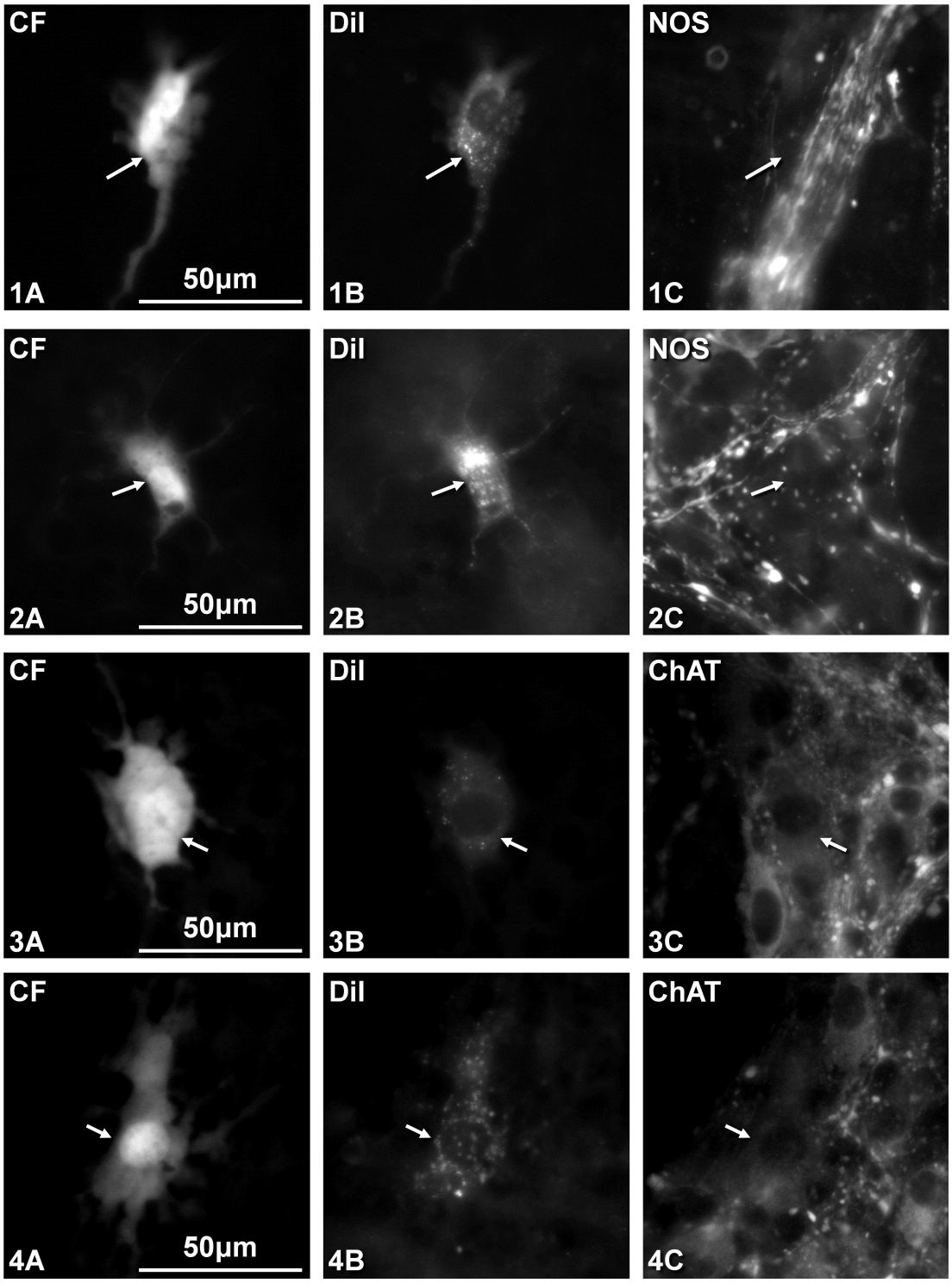


**Figure 6.11**

Micrographs of viscerofugal neuron cell bodies, matched horizontally. Micrographs show carboxyfluorescein (**1A**-**4A**), DiI (**1B**-**4B**) and immunoreactivity for nitric oxide synthase (**1C**-**2C**), or choline acetyltransferase (**3C**-**4C**). Note that viscerofugal neurons in **1** and **2** lacked immunoreactivity for nitric oxide synthase in their cell bodies. Viscerofugal neurons **3** and **4** contained immunoreactivity for choline acetyltransferase.

*Spatial distribution of NOS immunoreactive viscerofugal neurons*

Two-hundred and fifty-four DiI-labelled viscerofugal neurons were mapped and analysed for NOS immunoreactivity in 11 preparations (n=7, **figure 6.12**). One-hundred and five neurons contained NOS (41%) and 149 (59%) lacked NOS immunoreactivity. NOS-immunoreactive neurons were distributed in the circumferential axis more widely and further from the mesenteric border (105 cells, n=7) compared to viscerofugal neurons without NOS (149 cells, n=7), which were dense at the mesenteric border (mean distances from the mesenteric border: 1.5 ± 1.6mm vs 0.6 ± 1.1mm, respectively, $p<0.001$ independent samples t-test, n=6, **figure 6.12**). In addition, there were differences in the distributions of viscerofugal neurons with and without NOS immunoreactivity along the colon. As multiple nerve trunks in each preparation were labelled with DiI, the nerve trunks from which viscerofugal neurons were retrogradely labelled could not be confidently identified. Thus, we analysed the distribution of viscerofugal neuron cell bodies along the gut relative to the midline of preparations (half way between the oral and aboral end of the preparation). Viscerofugal neurons containing NOS immunoreactivity were distributed on average 1.7 ± 2.9mm oral to the midline of preparations. In contrast, viscerofugal neurons lacking NOS lay slightly aboral to NOS immunoreactive neurons, located on average 0.1 ± 2.8mm oral to the midline ($p<0.001$ independent samples t-test, **figure 6.12**).

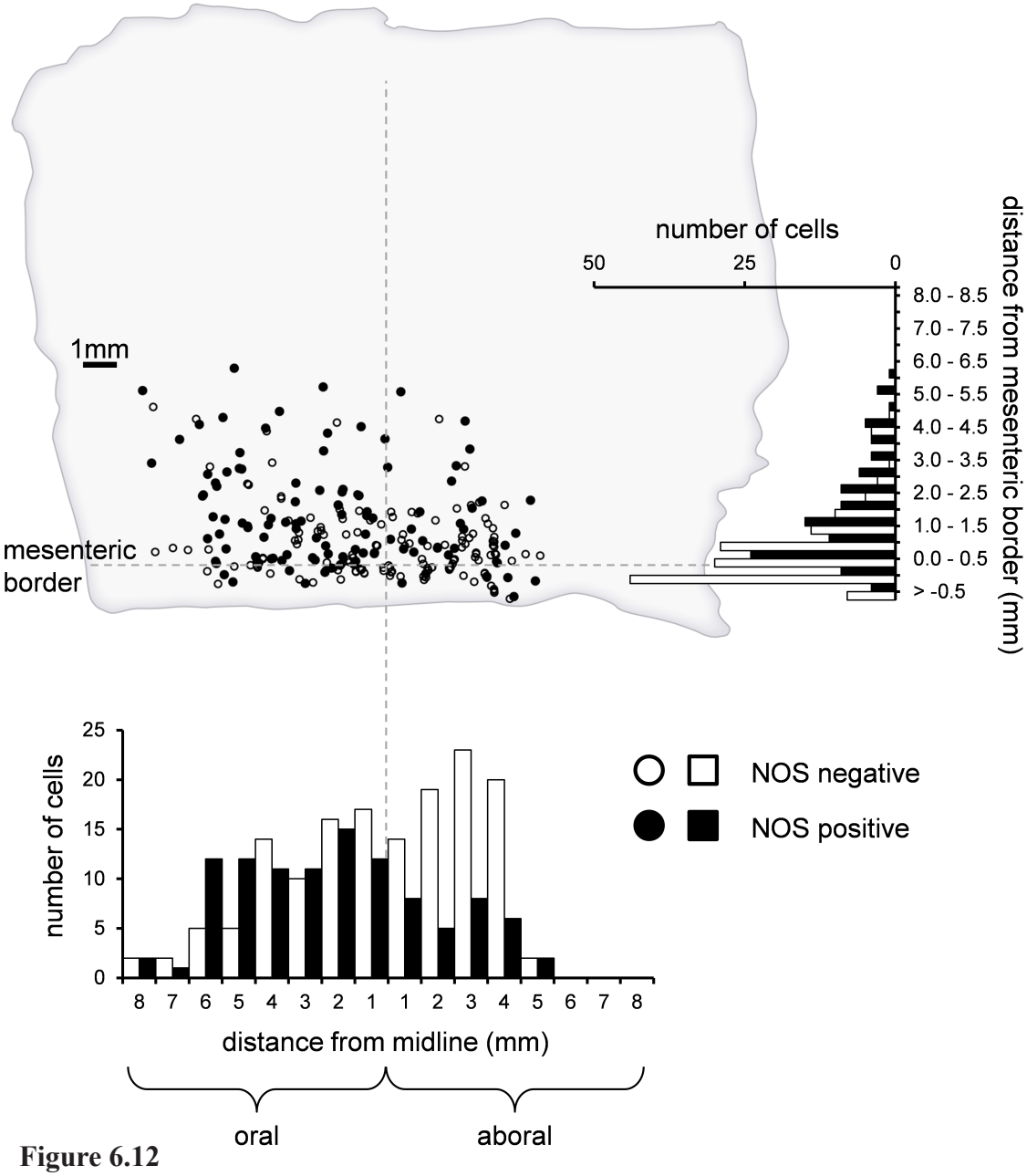


**Figure 6.12**

The spatial distribution of DiI-labelled viscerofugal nerve cell bodies with, and without immunoreactivity for nitric oxide synthase. This figure includes a composite map that shows the locations of retrogradely-labelled viscerofugal nerve cell bodies and whether they contained NOS immunoreactivity. NOS immunoreactive viscerofugal neurons are indicated as black squares on the composite map; viscerofugal neurons that lacked NOS are indicated as open grey circles. The frequency histograms adjacent the composite map show in graphical form the distributions of the two populations of viscerofugal neurons: NOS immunoreactive viscerofugal neurons are indicated as black bars; viscerofugal neurons lacking NOS immunoreactivity are shown as open white bars. Note the high density of the NOS negative population of viscerofugal neurons around the mesenteric border, shown in the frequency histogram with horizontal bars. NOS positive viscerofugal neurons were relatively more evenly distributed. See also the distributions of the two populations along the gut in the frequency histogram with vertical bars. NOS positive viscerofugal neurons were preferentially located oral to the midline. NOS negative viscerofugal neurons were more prominent on the aboral side.

*Impalements of viscerofugal neurons*

Thirty-nine viscerofugal neurons were impaled in 20 preparations that had been maintained in organ culture for 2-4 days (n=14). DiI-labelled neurons were reliably impaled; carboxyfluorescein labelling successfully correlated with DiI-labelled neurons in 39 of 42 cells. In 3 cases where labelling did not match, carboxyfluorescein-labelled neurons were found to partially overlie the targeted DiI-labelled neuron. Data from these 3 recordings were discarded. The mean resting membrane potential of viscerofugal neurons was -48 ± 4mV (16 cells) and input impedance was 128 ± 42MΩ (11 cells). The membrane time constant to 100pA hyperpolarizing current pulses near resting membrane potential was 8.1 ± 4.4ms (15 cells; **figure 6.13B**). Depolarizing current pulses evoked action potentials in 21 of 24 cells tested, 3 cells were inexcitable (10-500ms duration, 100-900pA). Several cells fired "anodal break" action potentials upon termination of imposed hyperpolarizations (6/24 cells; **figure 6.14**). The mean action potential amplitude was 57 ± 9mV (16 cells, mean overshoot 11 ± 7mV) and the duration of action potentials at half peak amplitude was 1.8 ± 0.4ms.

Viscerofugal neurons fired action potentials with instantaneous frequencies peaking at 80Hz, while the average maximum instantaneous frequency of action potential discharge was 49 ± 18Hz (18 cells). Continuous discharge of action potentials occurred in 8 cells in response to imposed depolarizations lasting 100-500ms (**figure 6.15**). The repetitive firing rate averaged over 500ms was 34 ± 11Hz (5 cells). In addition, there was an undershoot in membrane potential following repetitive action potential discharges evoked by a 500ms imposed depolarization (8.1 ± 3.9mV, 6.2 ± 4.7s duration, 300pA, 11 cells; the undershoot can be seen in **figure 6.15A** and

**6.15B**). Inflections on the repolarization phase of action potentials, a feature of AH neurons (Kunze et al., 1995), were not present in 20 of 21 cells that fired action potentials (**figure 6.13A**). However, in the single multipolar viscerofugal neuron (**figure 6.08**) there was a pronounced inflection on the repolarization phase of action potentials, followed by a long after-hyperpolarization (8-10mV, 5-8s, **figure 6.16A** and **6.16C**). In addition, a "sag" in membrane potential to hyperpolarizing pulses was evident in this one cell (**figure 6.16B**), typical of the cation $I_H$ current previously described in AH neurons (Galligan et al., 1990).

Post-hoc immunohistochemical characterisation indicated that the viscerofugal neurons with NOS immunoreactivity had depolarised membrane potentials compared with those lacking NOS immunoreactivity (-45.9 ± 3.2mV and -52.9 ± 1.6mV, respectively, 7 NOS+ cells, 2 NOS- cells). No other electrophysiological differences were observed between these classes of cell.

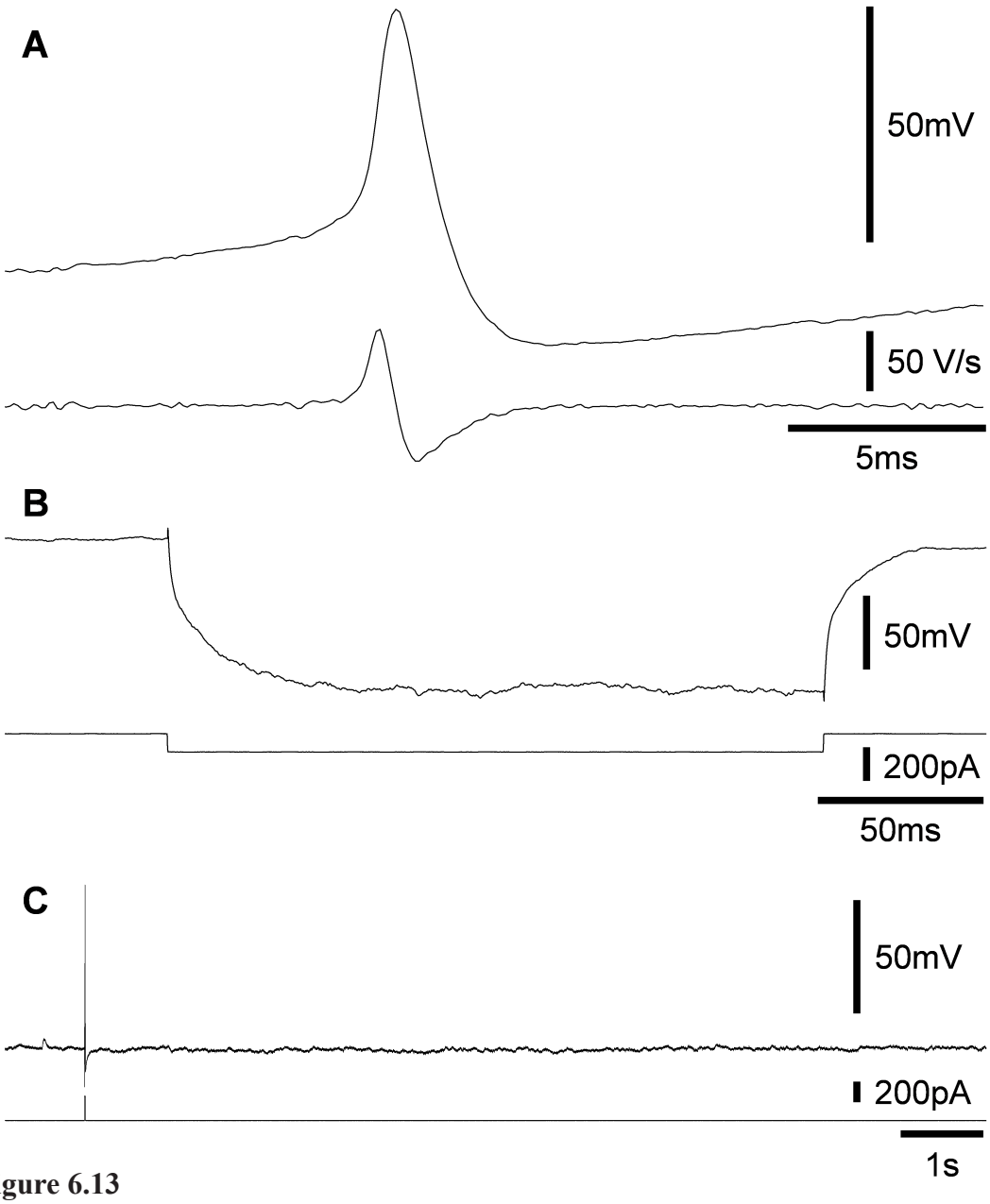


**Figure 6.13**

Electrophysiological characteristics of viscerofugal neurons. Shown in **A** is a voltage trace of an action potential in a viscerofugal neuron (upper trace). The first time derivative of the voltage is shown in the lower trace. Both traces show the action potential lacks an inflection on the falling phase of action potential. This was characteristic of action potentials in 20/21 impaled viscerofugal neurons tested with depolarizing current pulses. Shown in **B** is an example of a 100pA hyperpolarizing current pulse in a viscerofugal neuron. Time constants and input impedance were calculated from these small current pulses at resting potential (these were 8.1 ± 4.4ms, and 128 ± 42MΩ, respectively). In **C,** a single action potential was evoked by a 10ms imposed depolarization. Note the lack of a long after-hyperpolarization.

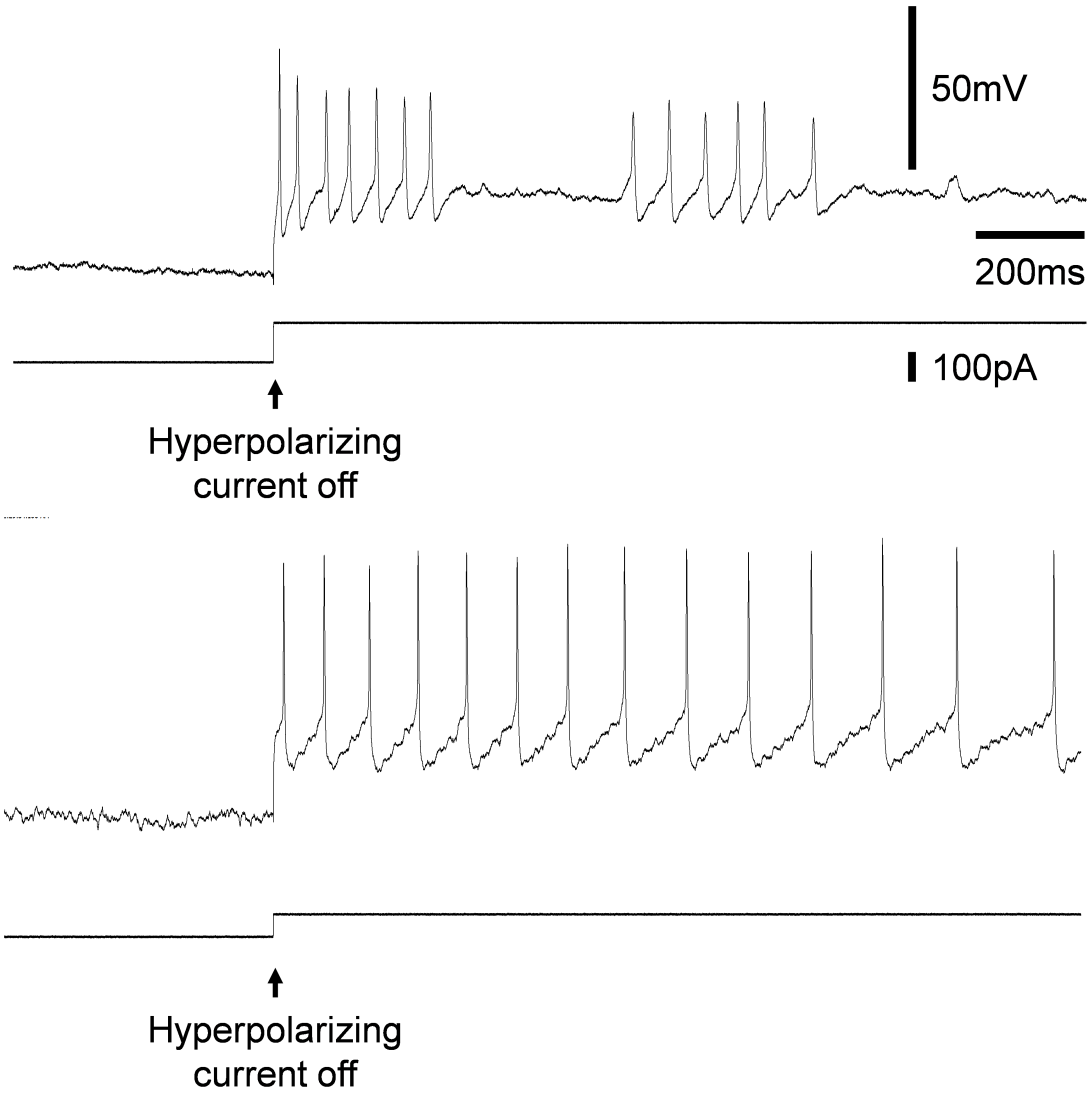


**Figure 6.14**

Anodal break action potentials. These traces show examples of anodal break action potentials that occurred in 6 of 24 viscerofugal neurons upon cessation of hyperpolarizing current pulses.

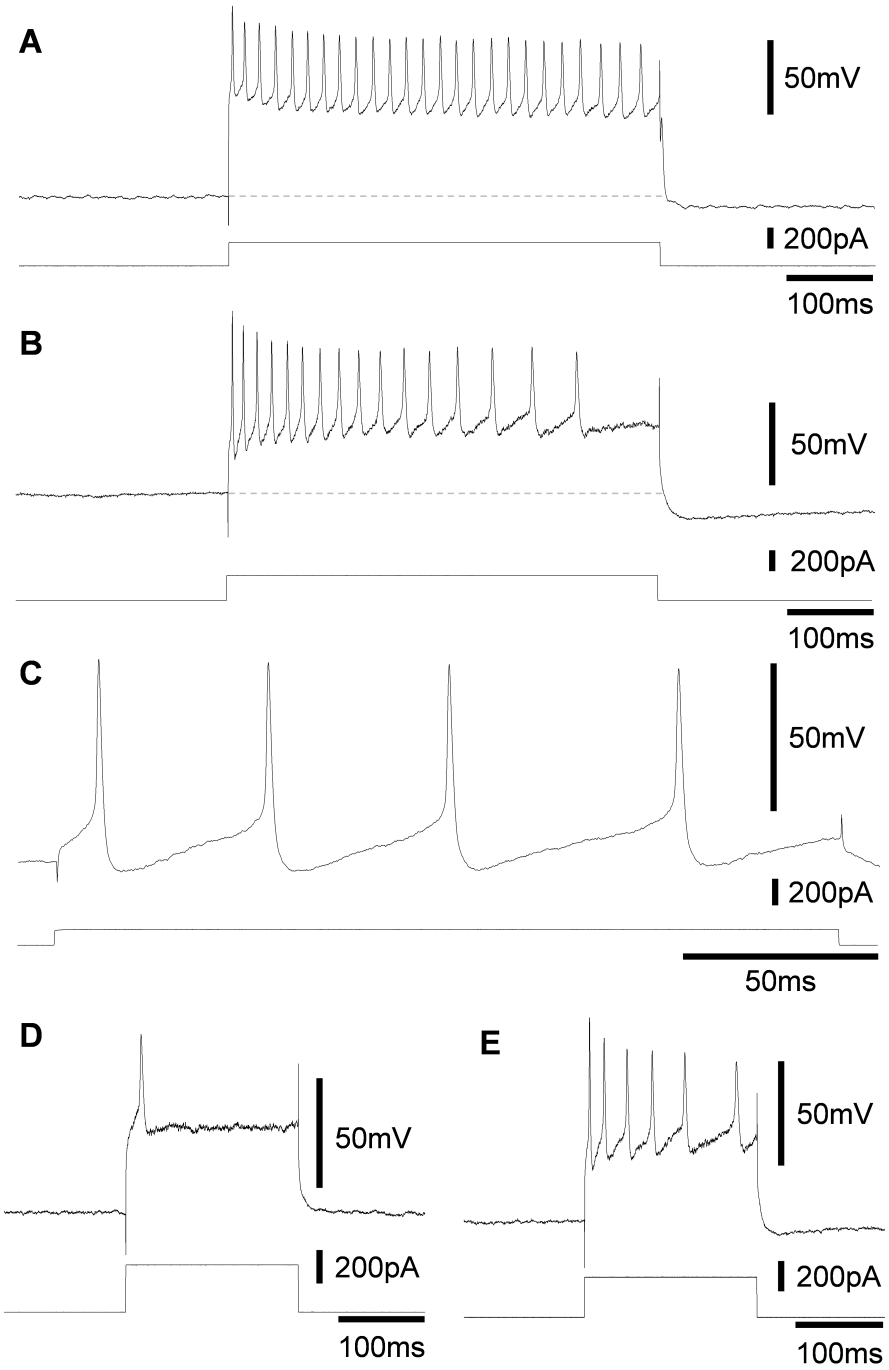


**Figure 6.15**

Firing behaviour in viscerofugal neurons. Shown in **A** and **B** are examples of repetitive firing throughout 500ms depolarizing current pulses. Note the small undershoot in membrane potential on removal of the depolarization (dashed lines) (**C**) Expanded trace of repetitive firing to a 200ms imposed depolarization. Examples of a single action potential and repetitive firing responses, evoked by 200ms depolarizing current pulses are shown in **D** and **E**, respectively.

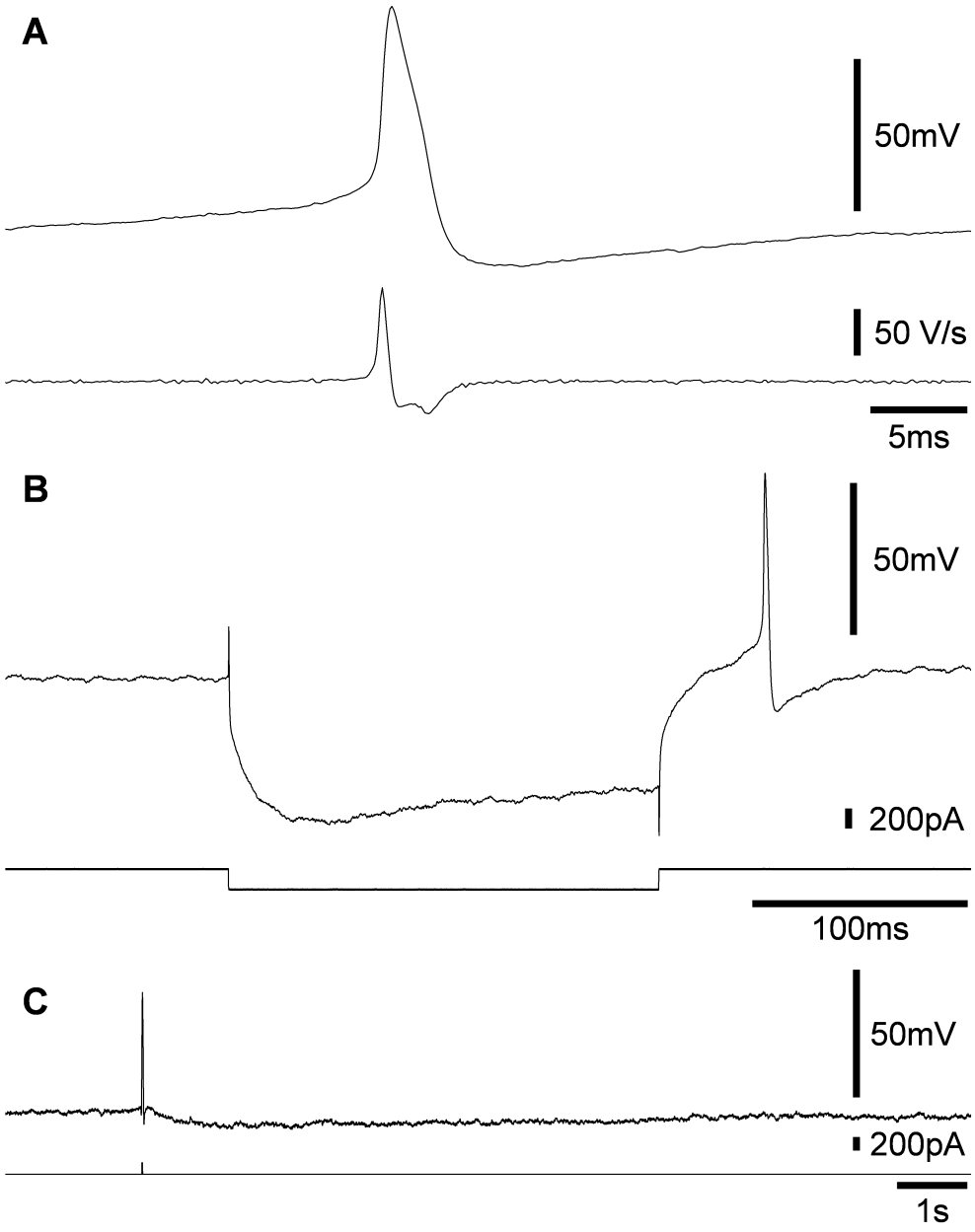


**Figure 6.16**

Electrophysiological characteristics of a single, multipolar viscerofugal neuron. Shown in **A** is a voltage trace of an action potential (upper trace) and the first time derivative of the voltage (lower trace). Note the shoulder on the falling phase of the action potential in the voltage trace, and also in the first time derivative of the voltage. In **B**, a 200pA hyperpolarizing current pulse activated an inward depolarizing current resulting in the appearance of a "sag" in the voltage trace. This is characteristic of the cation IH current, described in AH neurons. Also note the "anodal break" action potential at the offset of the hyperpolarizing current pulse. Shown in **C** is a long after-hyperpolarization that followed a single action potential evoked by a 10ms imposed depolarization.

*Relationship between firing behaviour and electrophysiological properties*

During recordings from viscerofugal neurons, it became clear that cells that fired more action potentials during depolarizing current pulses also tended to fire at higher frequency and had lower thresholds (measured by depolarizing current). The number of action potentials fired during a 500ms depolarizing current pulses was inversely correlated to the rheobase current (6.4 ± 7.7 action potentials, $r=-0.731$, $p<0.005$, 21 cells, n=12) and positively correlated with peak firing frequency ($r=0.661$, $p<0.01$, 16 cells, n=11). In addition, the half peak duration of action potentials was shorter in cells that fired at higher frequencies ($r=-0.622$, $p<0.01$, 21 cells, n=12).

*Spontaneous inputs and action potentials*

Spontaneous, ongoing fast EPSPs occurred in the majority of viscerofugal neurons, with a mean frequency of 0.5 ± 0.3Hz (30s samples, 28/33 cells, 85%, **figure 6.17A**). When tested, all ongoing EPSPs were abolished by hexamethonium (500μM, 1 cell, **figure 6.17C**). The mean amplitude of EPSPs near resting membrane potential was 6.2 ± 2.5mV (28 cells). In 7 cells, spontaneous action potentials occurred intermittently; in 2 cells regular firing occurred throughout the impalement (**figure 6.17B**). In these regularly firing cells, the frequency of firing was unaffected by hexamethonium (500μM; 2 cells, **figure 6.17D**), suggesting that firing was not caused by spontaneous nicotinic inputs.

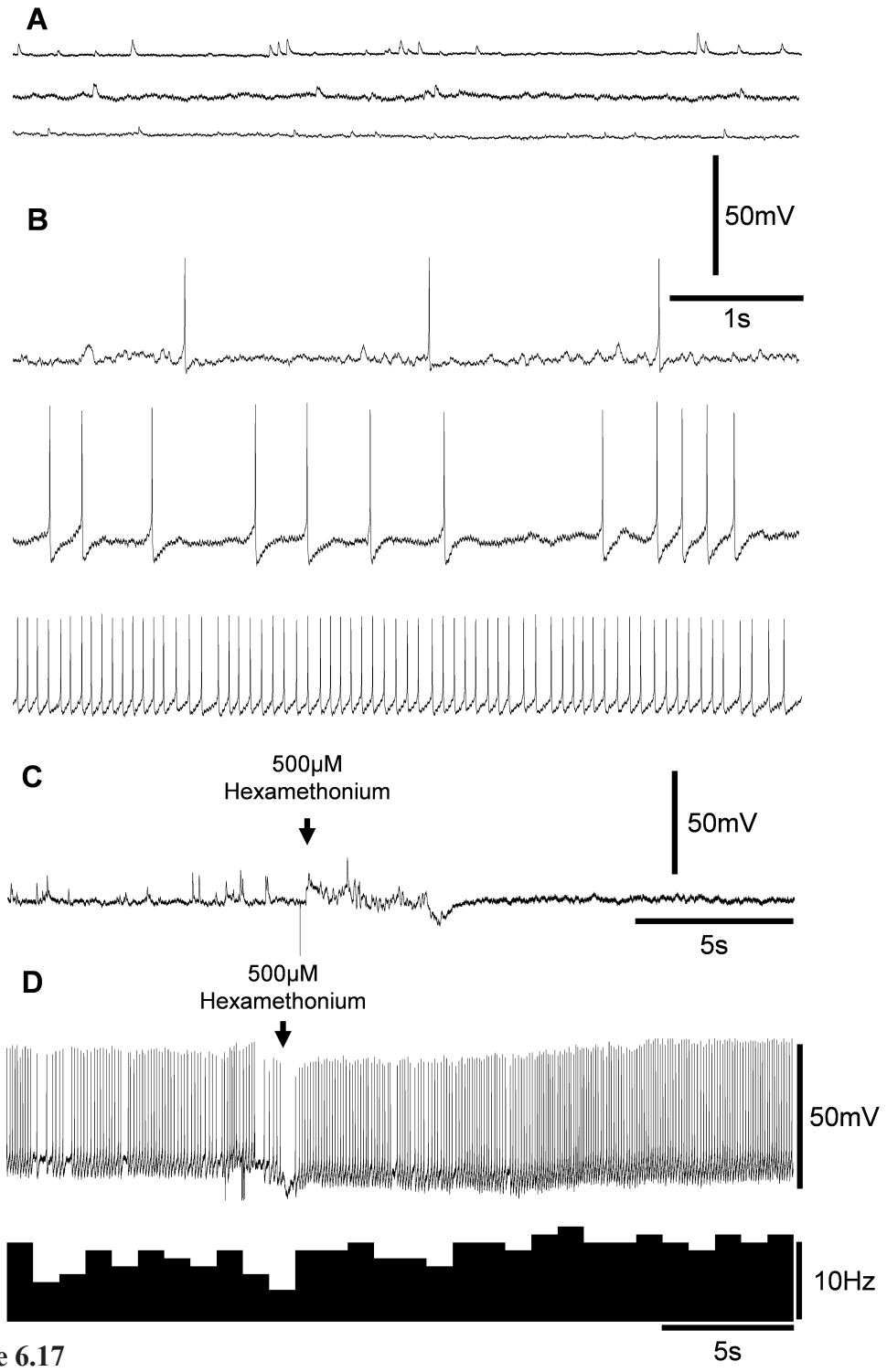


**Figure 6.17**

Spontaneous activity in viscerofugal neurons. Shown in **A** are example traces of ongoing spontaneous fast EPSPs from 3 different viscerofugal neurons. **B** shows examples of ongoing spontaneous action potential discharge in a further 3 viscerofugal neurons. All ongoing EPSPs were blocked by the nicotinic receptor antagonist hexamethonium (500µM); an example is shown in **C**. When applied during ongoing firing (example in **D**) the same concentration of hexamethonium failed to block ongoing firing in 2 neurons, suggesting that the action potentials in these neurons were not caused by nicotinic inputs.

*Circumferential electrical stimulation*

Single pulse electrical stimuli were applied to internodal stands 600 ± 100μm circumferential to each of the 24 impaled viscerofugal nerve cell bodies. In 19 cells (79%), circumferential electrical stimulation evoked fast EPSPs with a mean amplitude of 7.3 ± 3.2mV when measured close to their resting membrane potential (**figure 6.18A**). Five cells (21%) did not have fast EPSPs to circumferential electrical stimulation. Four of these five cells nevertheless had spontaneous EPSPs, consistent with S-neuron electrophysiological characteristics. The single cell that had neither spontaneous nor electrically stimulated EPSPs was the single multipolar viscerofugal neuron (**figure 6.08**).

Fast EPSP amplitude increased during hyperpolarizing current pulses in all cells tested. The extrapolated reversal potential averaged -4 ± 10mV (8 cells, n=7). In most cases, electrical stimulation of internodal strands evoked single EPSPs (11 cells, **figure 6.18A**). However, multiple EPSPs with different time-courses were evoked in 8 cells (2-4 peaks), suggesting polysynaptic input pathways. In 7 cells, electrically stimulated EPSPs were suprathreshold and evoked 1-2 action potentials (**figure 6.18B**).

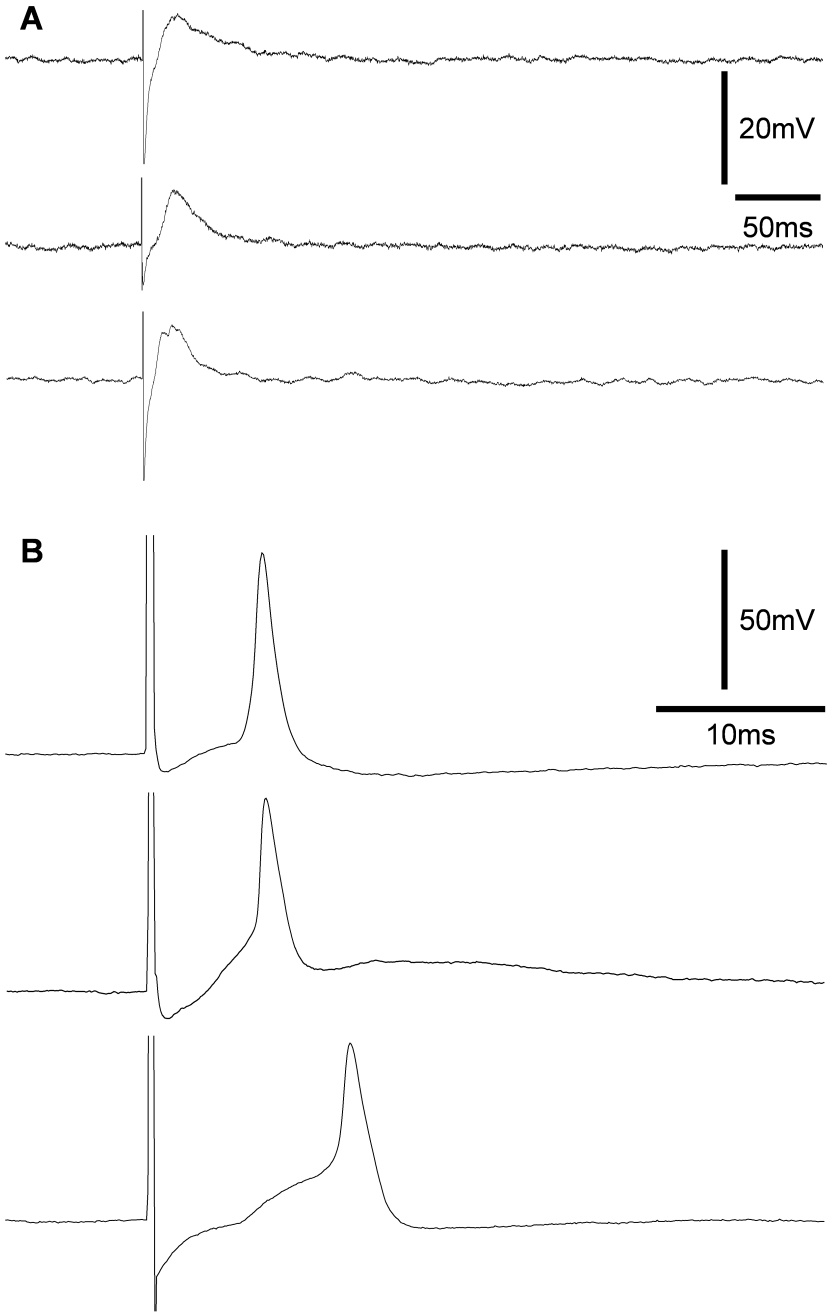


**Figure 6.18**

Electrical stimulation of internodal strands. Internodal strands were stimulated about 0.6mm from the recorded viscerofugal nerve cell bodies. Shown in **A** and **B** are examples from 6 different viscerofugal neurons of the evoked fast EPSPs that were subthreshold (**A**) and suprathreshold (**B**).

*Direct pharmacological stimulation of viscerofugal neurons*

Action potentials evoked by electrical stimulation may propagate orthodromically or antidromically along axons to synaptic release sites and therefore cannot be used to define the neuron's source of presynaptic inputs. To avoid this problem, we activated presynaptic inputs to impaled viscerofugal neurons with focal pressure-ejected pulses of DMPP (10μM) to reveal the sites of cell bodies of enteric neurons that synapsed onto viscerofugal neurons. We first tested DMPP ejection directly onto the recorded viscerofugal nerve cell body, to characterize the effect of a nicotinic receptor agonist on enteric neurons. When applied directly, DMPP ejection evoked large depolarizations in viscerofugal neurons (23 ± 10mV; 21/22 cells), starting after an average delay of 350 ± 230ms. The duration and decay time constant from peak amplitude of DMPP-evoked depolarizations was 4.4 ± 3.7s and 2.5 ± 2.4s, respectively. The time-course of DMPP-evoked depolarizations were readily distinguished from spontaneous EPSPs, which were of lower amplitude and shorter duration (6.2 ± 2.5mV, duration 34 ±16ms and decay time constant from peak amplitude 14 ± 7ms, 28 cells). Action potentials were often superimposed upon DMPP-evoked depolarizations (1-23 action potentials, maximum instantaneous frequency 30 ± 10Hz; 8 cells, see **figure 6.19**). The single cell that was not depolarized by 10μM DMPP was the multipolar Dogiel type II neuron shown in **figure 6.08** (as previously reported in AH neurons; Morita et al., 1982). The depolarizing effect of DMPP applied directly onto the recorded viscerofugal nerve cell body was blocked by 500μM hexamethonium (6 pulses, n=1). In addition, pressure ejection of Krebs and dye solution without DMPP, directly onto the recorded viscerofugal nerve cell body, had no effect on membrane potential (2 pulses, n=1).

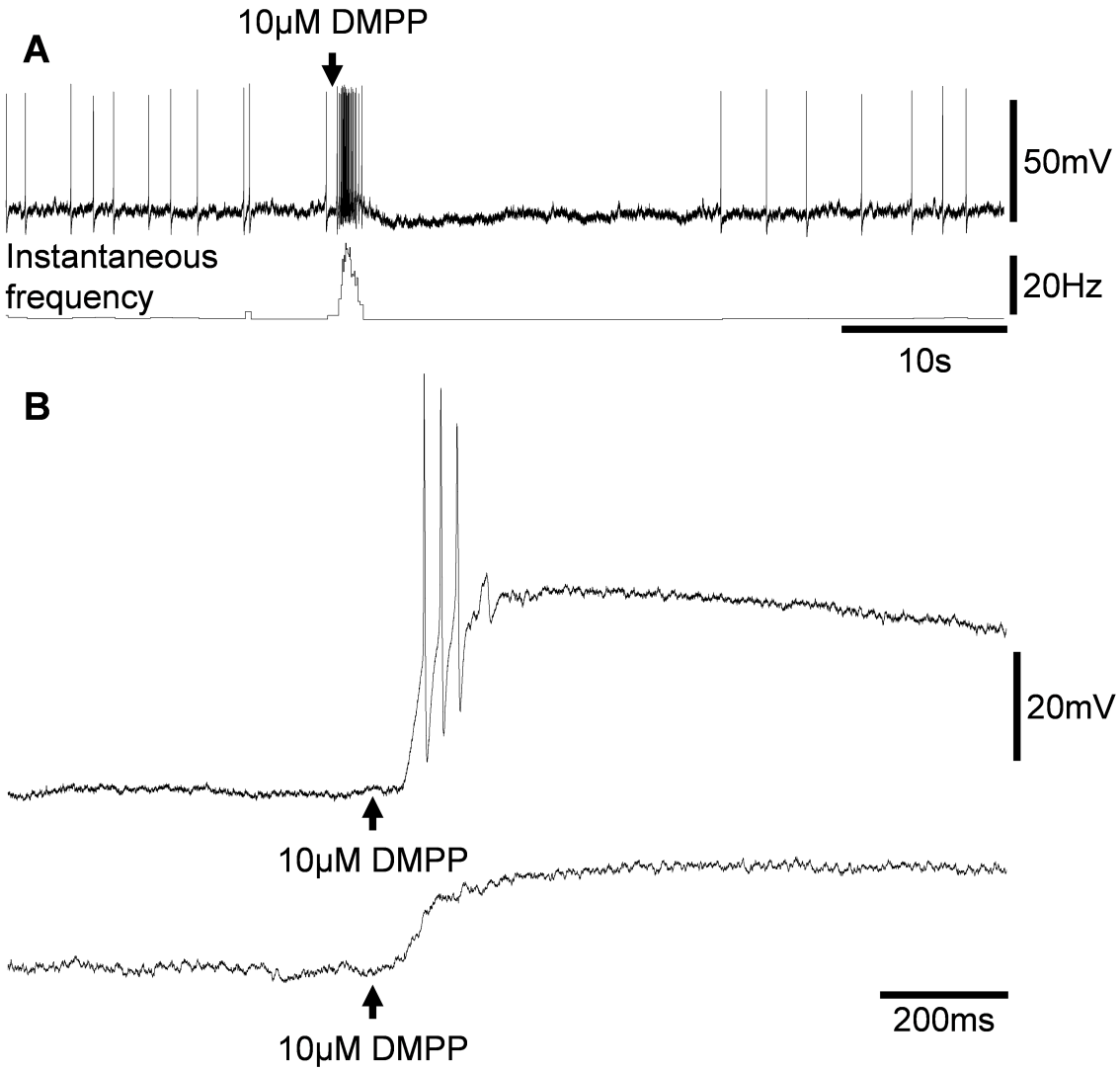


**Figure 6.19**

Effect of nicotinic receptor agonist (DMPP) pressure-ejected directly onto viscerofugal nerve cell bodies. Shown in **A** is a burst of action potentials evoked by DMPP up to a peak instantaneous frequency of around 20Hz. (**B**) Expanded time-course of membrane potential responses to DMPP. The latency from ejection to peak depolarization was 350 ± 230ms (21 cells). Note that several action potentials occur on the depolarization phase in the upper trace.

*Pharmacological stimulation of synaptic input to viscerofugal neurons*

Synaptic inputs to impaled viscerofugal neurons were activated by focal pressure-ejected pulses of DMPP (10μM) to reveal the sites of cell bodies of enteric neurons that synapse onto viscerofugal neurons. Their locations were then mapped. DMPP was applied to many sites up to 3mm from impaled, DiI-labelled viscerofugal neurons, including sites in myenteric ganglia and internodal strands (394 sites; 189 oral, and 204 aboral to the impaled nerve cell bodies). In none of 46 internodal strands did DMPP evoke any synaptic inputs to a viscerofugal neuron, suggesting that DMPP did not excite axons-of-passage. The majority of sites tested with DMPP produced no measureable change in membrane potential of the recorded viscerofugal neuron (310/348 myenteric ganglia). However, in some myenteric ganglia, DMPP application evoked fast EPSPs in viscerofugal neurons that were repeatable (**figure 6.20** and **6.21**), with a response delay comparable to direct stimulation of action potentials (38 ganglia, 10/16 cells tested, latency 300 ± 316ms). Examples are shown in **figure 6.22** and **6.23**. DMPP activated inputs from sites either oral or aboral to viscerofugal neurons in approximately equal numbers and spatial distribution within the areas tested (19 descending, 19 ascending; see **figure 6.24** shows a map of all sites that were tested with DMPP). Most inputs were located 0.5-0.75mm from the impaled viscerofugal nerve cell body (**figure 6.25**). Pressure ejection of control solution (Krebs with dye) onto myenteric ganglia had no effect on membrane potential (14 sites, n=1).

In most cases, DMPP applied to a remote site in plexus evoked a single EPSP in the recorded viscerofugal neuron (25/37 sites). At some sites, multiple EPSPs summated, generating a compound depolarization with several discrete peaks (12 sites, 2-5

peaks, **figure 6.20** and **6.21**). The delay between separate peaks corresponded to a maximum instantaneous firing rate of 48 ± 29Hz (range 5-90Hz) which is compatible with a single presynaptic neuron firing repetitively, although it is possible that inputs could have arisen from more than one presynaptic neuron within the same ganglion. Instances of single and multiple EPSPs were seen from ascending and descending pathways (11 and 14 single inputs from descending and ascending sources, respectively, and 8 and 4 multiple inputs from descending and ascending sources, respectively, NS, $X^2$ test). In some instances, DMPP-activated synaptic inputs reached threshold for action potentials (2 ascending, 2 descending). Occasionally, trains of fast EPSPs were evoked a few seconds after application, suggesting that polysynaptic pathways had been activated (**figure 6.26**). The average amplitude of DMPP-evoked EPSPs at resting membrane potential was 7.5 ± 5.4mV (11 inputs, 5 cells). In 6 cells, inputs were identified both oral and aboral to the recorded nerve cell body (n=6). Fast EPSPs from descending inputs were consistently greater in amplitude than ascending inputs, when compared at the same holding potential (current ranged 0 to -180pA; 13 oral inputs, 13.1 ± 4.3mV vs. 14 aboral inputs, 10.1 ± 4.8mV, respectively, $p<0.05$, paired t-test). Krebs/dye without DMPP never evoked EPSPs when applied to ganglia (14/14 sites, 1 cell). No correlation was found between the presence of synaptic inputs to any given viscerofugal neuron and the presence of NOS immunoreactivity in the same neuron. However, NOS immunoreactive cells tended to have more inputs (2.9 inputs per cell, 12 cells) than cells without NOS (0.8 inputs per cell, 4 cells), but the difference was not significant, possibly because of the small sample ($p=0.16$, t-test).

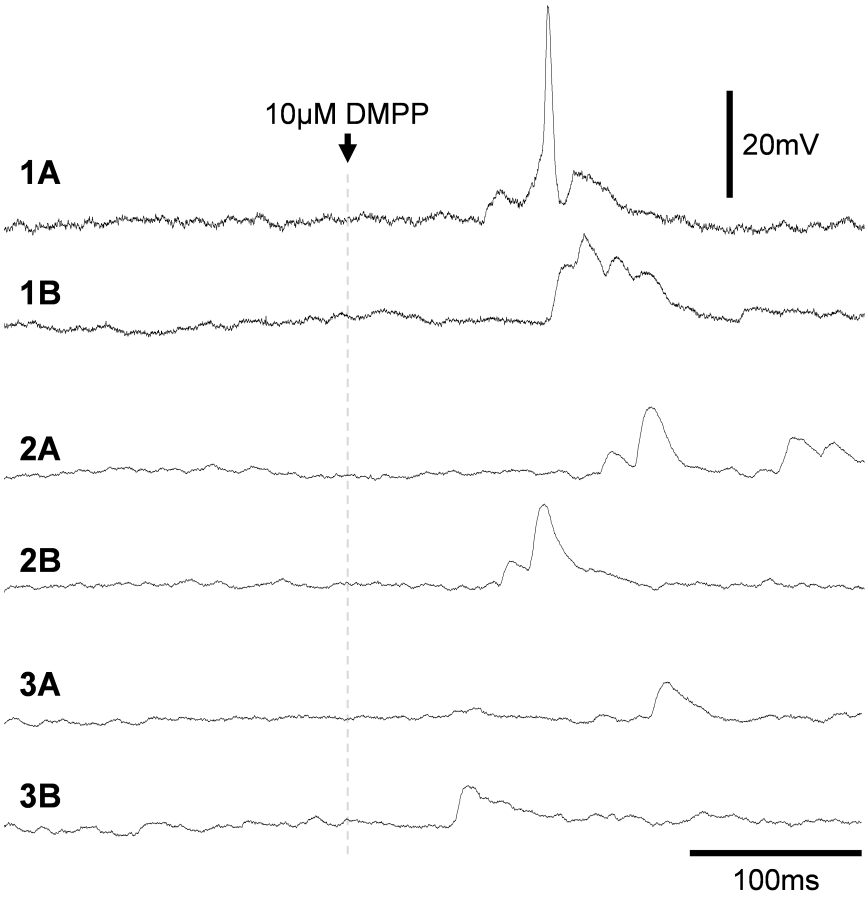


**Figure 6.20**

DMPP-evoked synaptic responses in viscerofugal neurons: matched examples of fast EPSPs evoked by DMPP applied to parts of myenteric ganglia. These traces show examples of repeated applications of DMPP onto the same myenteric ganglion. On repeat applications, DMPP often gave rise to similarly shaped fast EPSPs in the recorded viscerofugal nerve cell body. This occurred with single and multiple, compound fast EPSPs. Here, repeated synaptic responses to stimulation of 3 different myenteric ganglia are shown (**1A** and **1B**; **2A** and **2B**; and **3A** and **3B**). In some cases, fast EPSPs were suprathreshold (as in **1A**). Note that there are differences in the latencies of evoked fast EPSP between repeated applications. This was most likely caused by differences in the position of the pipette tip, which was moved between repeated applications in order to test other sites on the tissue. The similarity of the synaptic responses between repeat applications of DMPP suggests that the same synaptic terminals were activated.

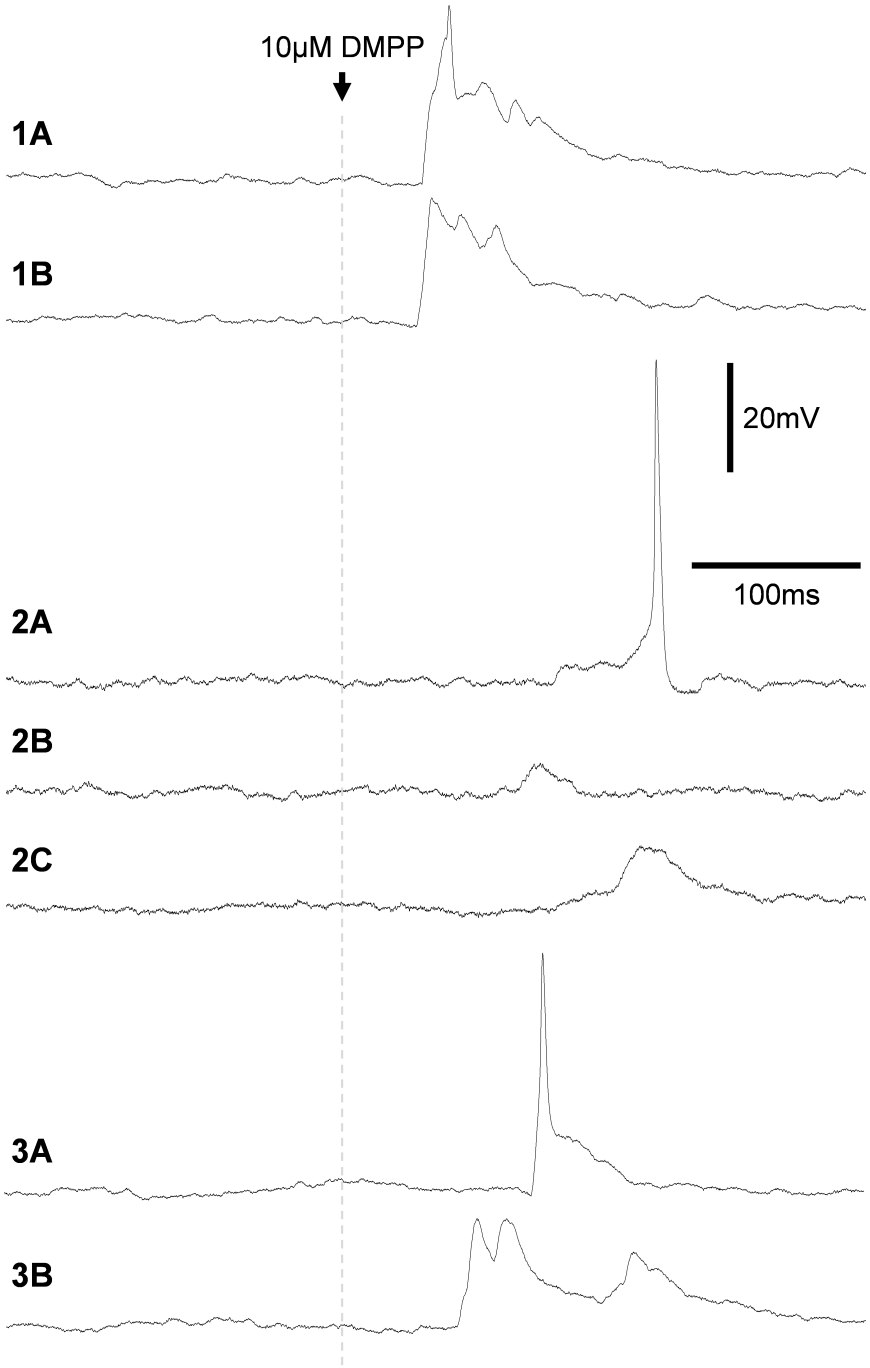


**Figure 6.21**

DMPP-evoked synaptic responses in viscerofugal neurons: matched examples of fast EPSPs evoked by DMPP applied to parts of myenteric ganglia. This figure includes further examples of repeated DMPP-evoked fast EPSPs in viscerofugal neurons. Each set of repeated fast EPSPs were evoked by DMPP applied to the same myenteric ganglion (**1A** and **1B**; **2A**-**2C**; and **3A** and **3B**).

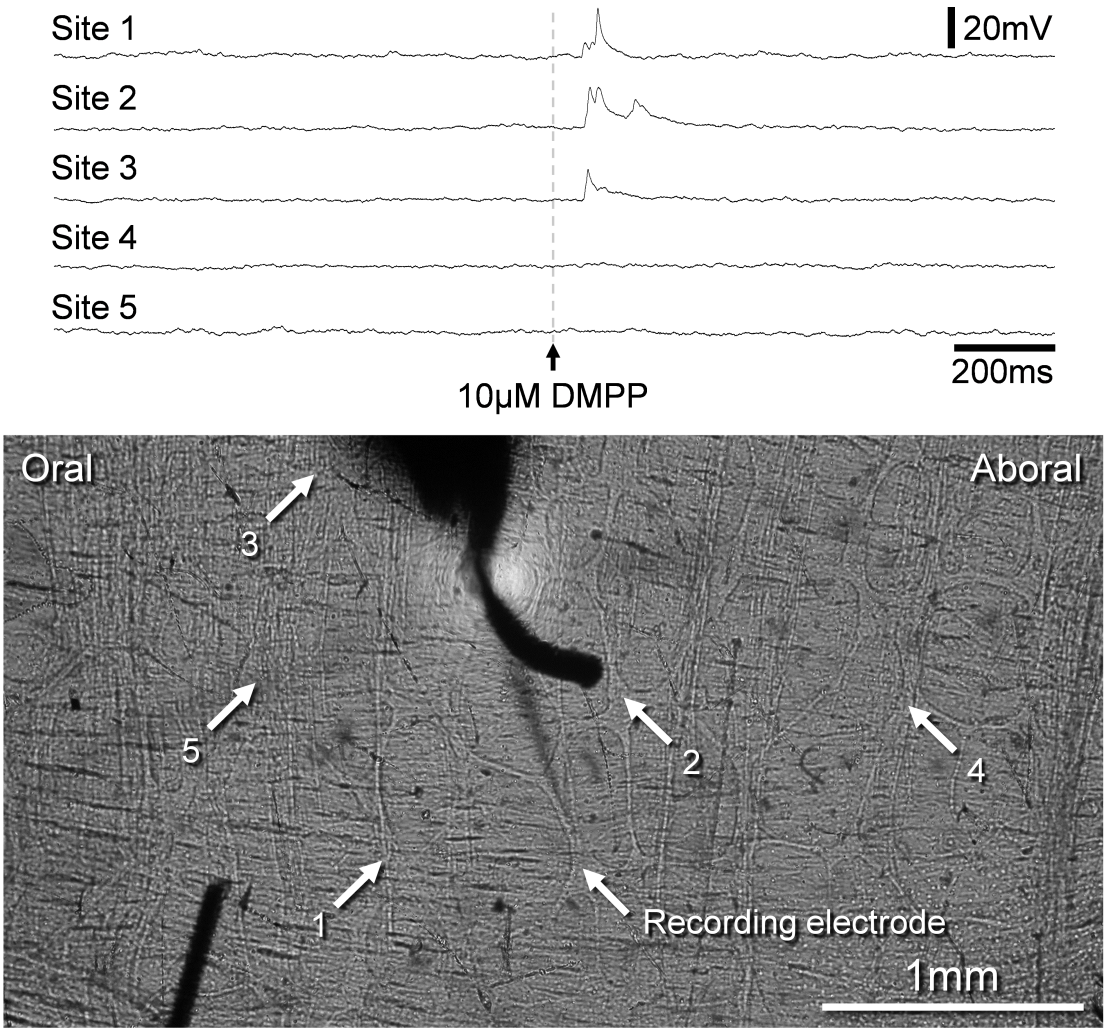


**Figure 6.22**

Localization of enteric neurons that provide fast synaptic inputs to viscerofugal neurons. This figure shows example membrane potential responses to pressure ejection of DMPP at sites around an impaled viscerofugal neuron. These examples show the effects of DMPP ejection onto 5 different sites of the preparation, corresponding to the numbered positions on the photomicrograph of the preparation. Single and multiple-peak fast EPSPs were evoked at sites 1-3. However at sites 4 and 5 there were no measurable responses. In total there were 26 sites tested in this preparation, revealing 8 synaptic inputs to the recorded viscerofugal nerve cell body (located at the tip of the recording electrode).

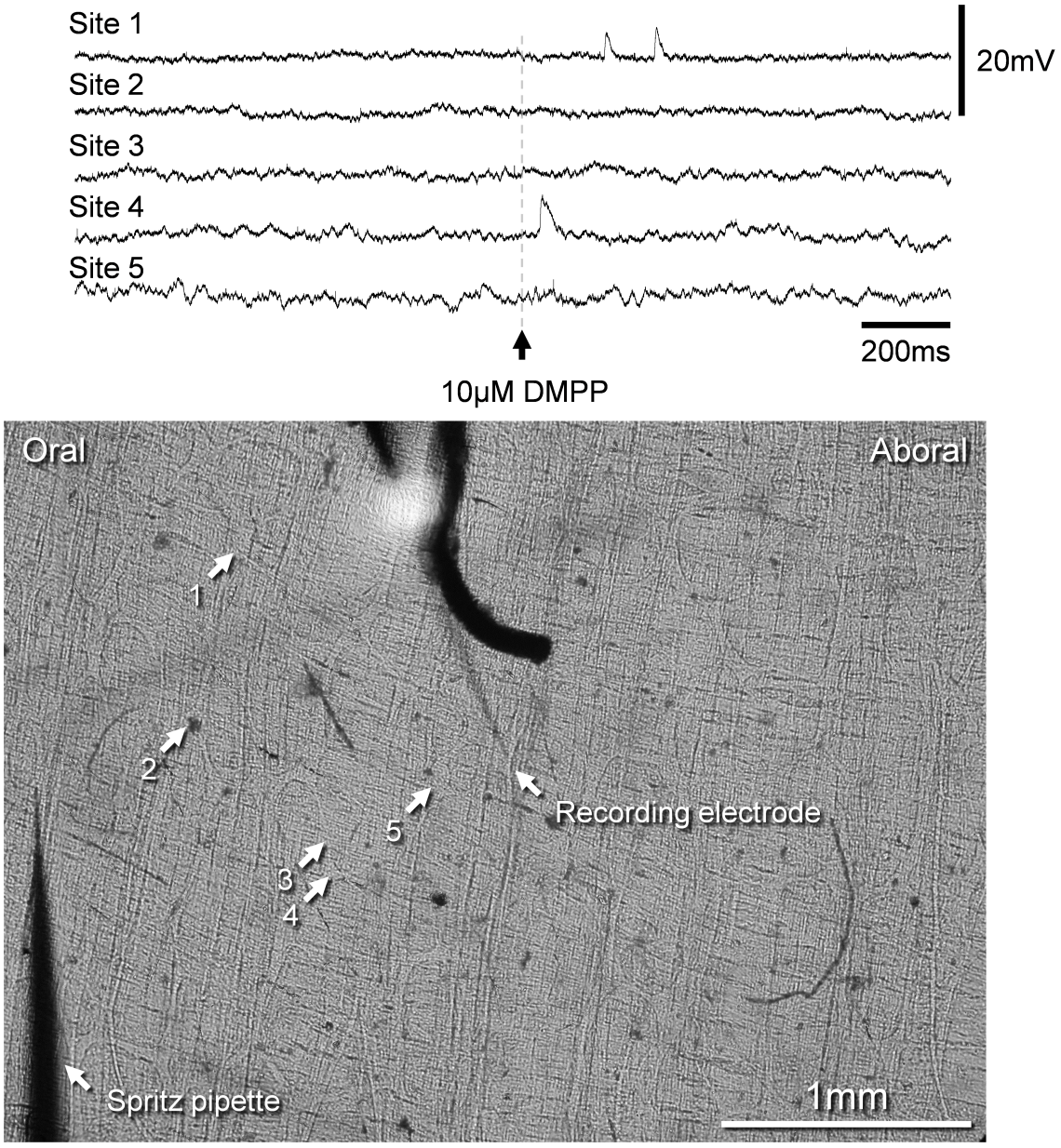


**Figure 6.23**

Localization of enteric neurons that provide fast synaptic inputs to viscerofugal neurons. This figure shows examples of membrane potential responses to pressure ejection of DMPP at sites around an impaled viscerofugal nerve cell body. In this example, DMPP ejected at sites 1 and 4, gave rise to fast EPSPs in the recorded viscerofugal nerve cell body. When DMPP was ejected onto site 3, an internodal strand close to site 4, no detectable response was evoked. DMPP ejected onto sites 2 and 5 (both parts of myenteric ganglia) also did not evoke detectable membrane responses in the recorded viscerofugal nerve cell body. Note that the recorded viscerofugal nerve cell body in this example is located at the shadow of the tip of the recording electrode shown in the photomicrograph (arrow). The shadow of the micropipette used for ejecting DMPP can also be seen in the photomicrograph.

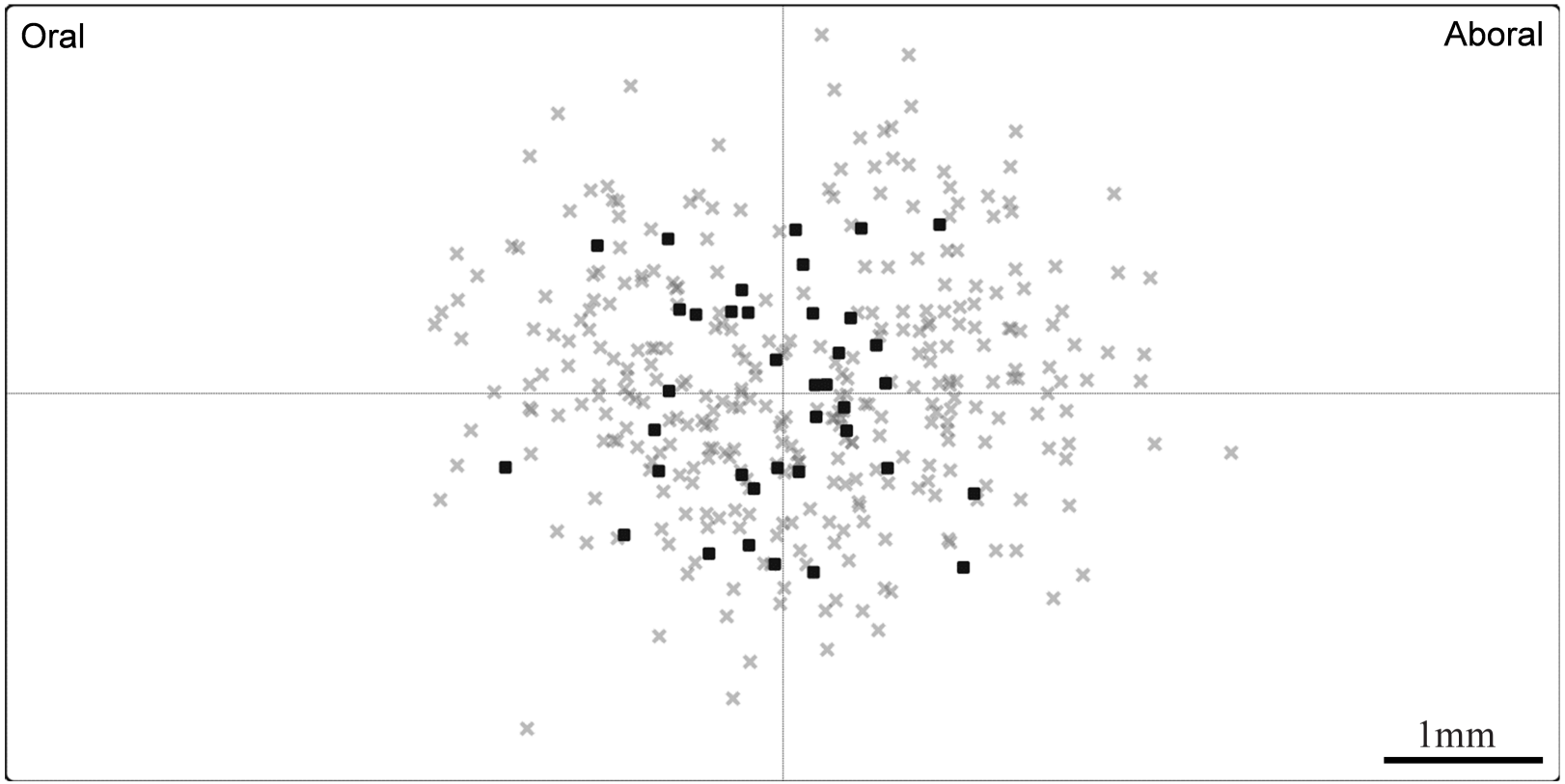


**Figure 6.24**

Composite map of all the sites upon which DMPP was ejected (394 total). These were recorded in 16 viscerofugal neurons. The location of all viscerofugal nerve cell bodies is set at the origin. The grey crosses indicate sites where DMPP-ejection gave no measurable responses in the recorded viscerofugal nerve cell body. The black squares indicate sites at which DMPP repeatedly evoked fast EPSPs in the recorded viscerofugal nerve cell body. In total, there were 38 DMPP-evoked synaptic inputs; 19 were located oral, and 19 were located aboral, to the recorded viscerofugal nerve cell bodies.

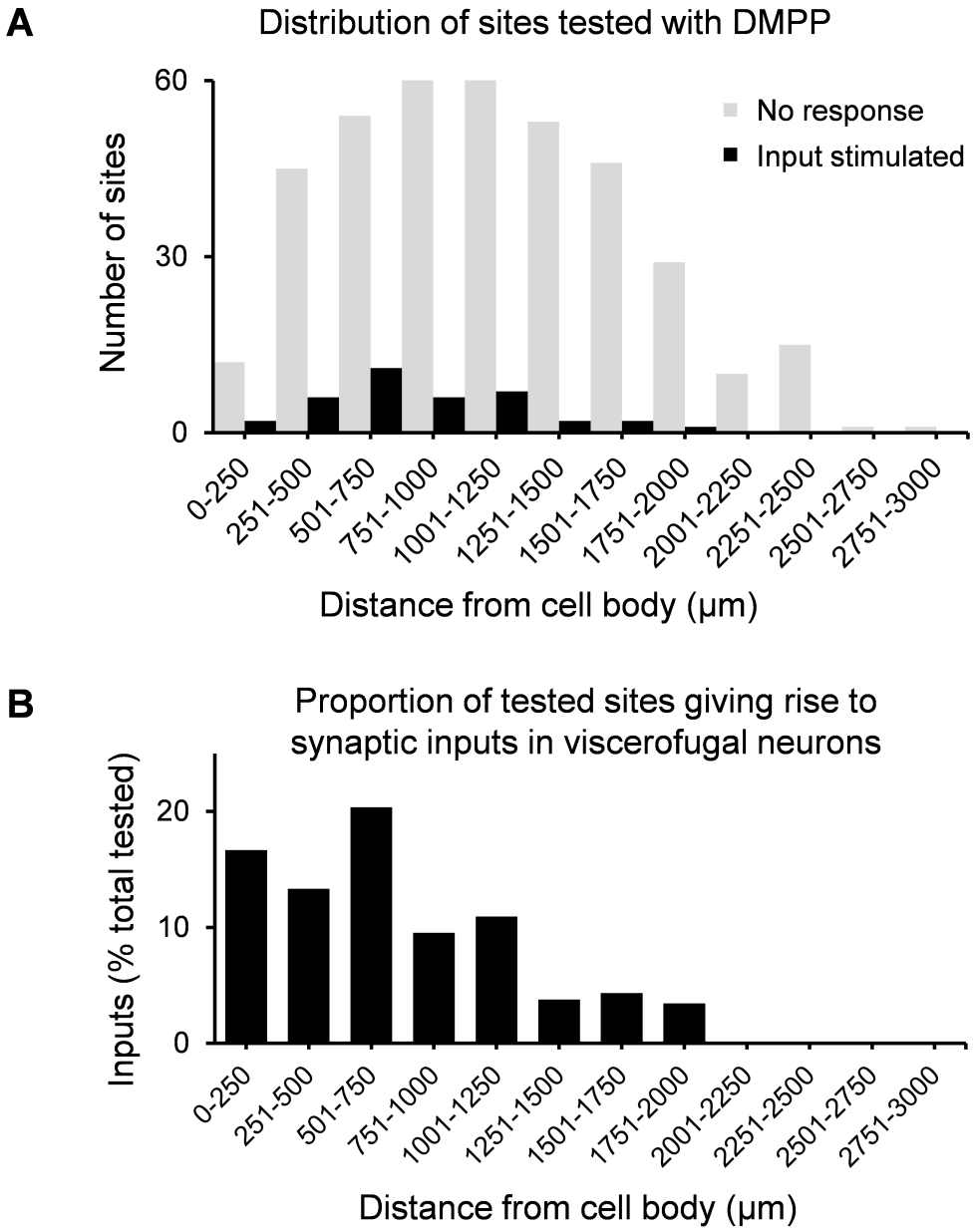


**Figure 6.25**

The distribution of sites tested with DMPP application. (**A**) Paired frequency histograms of the spatial distribution of sites tested with DMPP, and sites where DMPP evoked synaptic inputs. Note that most of the inputs were evoked from ganglia located 0.5-0.75mm from the recorded viscerofugal nerve cell body. Shown in **B** is the proportion of sites tested with DMPP that gave rise to repeatable fast EPSPs. The highest proportion of sites from which inputs were stimulated (over 20%) were ganglia located between 0.5 and 0.75mm from the recorded viscerofugal nerve cell body.

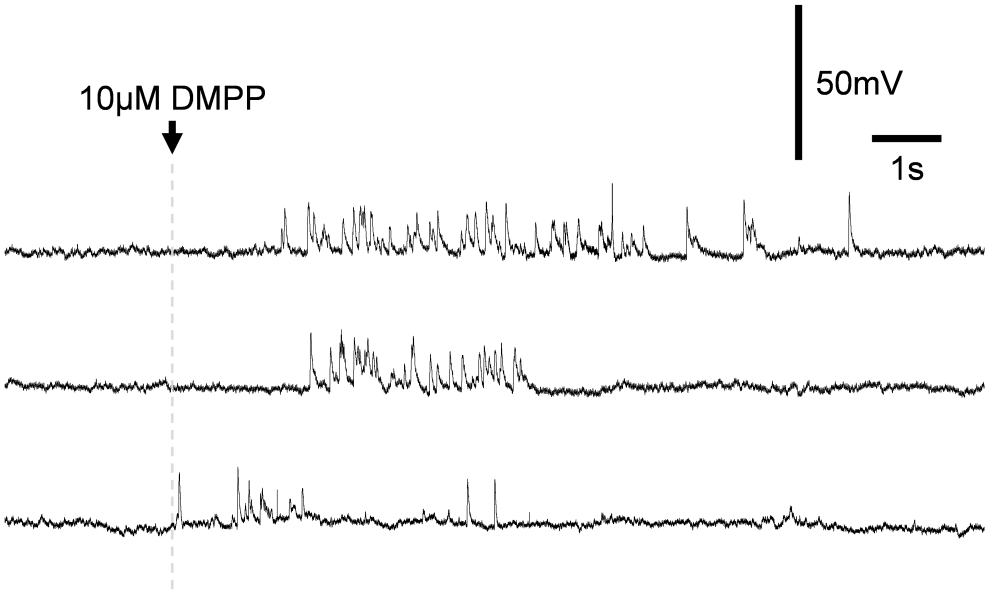


**Figure 6.26**

Trains of fast EPSPs, recorded in a viscerofugal nerve cell body that were evoked by DMPP ejection onto a myenteric ganglion. Occasionally, DMPP-ejection onto myenteric ganglia evoked trains of fast EPSPs that lasted several seconds. These typically occurred after several seconds delay. This activity suggests that polysynaptic pathways that supply inputs to the recorded viscerofugal nerve cell body were activated.

# DISCUSSION

*Viscerofugal neurons receive input from multiple enteric pathways*

Mapping of inputs to viscerofugal neurons by focal application of DMPP revealed that many myenteric neurons that synapse onto viscerofugal neurons were located close to their target neuron, in ganglia both orally, and aborally. This suggests that viscerofugal neurons receive synaptic inputs from multiple converging enteric pathways. The relative strength of presynaptic inputs from aborally-directed pathways (ie: from myenteric neurons located oral to the recorded viscerofugal nerve cell body) was consistently greater than inputs arising from cells located aborally. This is consistent with a previous morphological study in which it was reported that a greater proportion of cholinergic varicosities onto viscerofugal neurons arise from descending sources than from ascending pathways (Lomax et al., 2000). Most synaptic inputs to viscerofugal neurons were in local myenteric ganglia, 0.5- 1.0 mm from their cell body, suggesting their axons make synaptic contacts relatively close to their cell bodies. This is compatible with studies in guinea pig small intestine which show that many of the neurons that contribute to cholinergic and noncholinergic EPSPs arise from ganglia less than 1-2 mm away (Bornstein et al., 1984, LePard and Galligan, 1999). This result does not exclude the possibility that larger ascending and descending pathways may also converge onto viscerofugal neurons. The size of preparations in the present study prevented this from being tested systematically.

*DMPP stimulation of myenteric S-neurons*

Viscerofugal neurons, which correspond electrophysiologically to myenteric S-neurons, were depolarized and fired action potentials when DMPP was applied directly to their cell bodies. We assume that DMPP caused similar activation of other classes of myenteric S-neurons. If other myenteric neurons synapsed onto the recorded viscerofugal neuron, then DMPP activation should evoke discrete fast EPSPs. Viscerofugal neurons are pharmacologically activated by low pressure application of 5µl DMPP boluses from a hand-held pipette (Hibberd et al., 2012c). To test whether the jet of fluid pressure ejected from a micropipette could mechanically activate viscerofugal neurons in the present study, we tested Krebs control solution, or DMPP solution in the presence of hexamethonium (500µM). Direct ejection of the fluid onto two impaled viscerofugal nerve cell bodies did not evoke detectable changes in membrane potential (8 pulses). Regular ejection of DMPP always depolarized impaled viscerofugal neurons when applied directly, except in the single multipolar viscerofugal neuron (21/22 cells). This suggests DMPP activated viscerofugal neurons via nicotinic receptors, rather than via mechanical activation by the fluid jet during DMPP ejection, despite the fact that they have been shown to be directly mechanosensitive (Hibberd et al., 2012c). Similar results were obtained in extracellular recordings of viscerofugal neurons using the same method of delivery; they were activated by DMPP but not Krebs control solution applied onto the same site (Hibberd et al., 2012c). This method of tracing sources of inputs has been used previously, with comparable results, to characterise orally-directed pathways onto ascending interneurons in the small intestine (Brookes et al., 1997a). As reported in the previous study (Brookes et al., 1997a), synaptic input could be evoked by DMPP applied focally to myenteric

ganglia, but not when applied to internodal strands. This suggests that DMPP initiates action potentials from nerve cell bodies rather than from fibres-of-passage and thus can be used to identify the sources of synaptic inputs.

*Direct electrophysiological recordings of identified viscerofugal neurons*

Extracellular recordings (Hibberd et al., 2012a) and intracellular recordings (Sharkey et al., 1998) of identified viscerofugal neurons have been made previously in fresh specimens of guinea pig colon, and in organ cultured preparations (Hibberd et al., 2012b). Intracellular recordings directly demonstrated that viscerofugal neurons receive fast excitatory synaptic inputs (Sharkey et al., 1998). The importance of fast EPSPs for the excitation of viscerofugal neurons was shown by the observation that pharmacological blockade of nicotinic synapses in the gut wall reduced both spontaneous and stretch-evoked output of viscerofugal neurons in prevertebral sympathetic ganglia (Crowcroft et al., 1971b, Bywater, 1993, Stebbing and Bornstein, 1993). The present study extends this finding and shows that viscerofugal neurons receive fast EPSPs from local myenteric neurons located both orally and aborally.

In the present study, viscerofugal neurons were retrogradely labelled by the fluorescent dye, DiI, after application to colonic nerves in organ cultured guinea pig distal colon. Targeted impalements of these neurons revealed passive electrophysiological characteristics similar to those reported by Sharkey (1998). Preservation of electrophysiological properties in DiI-labelled neurons after organotypic culture has been reported for colonic AH neurons (Neunlist et al., 1999),

ileal Dogiel type II cells (Brookes et al., 1995) ascending interneurons (Brookes et al., 1997a) and descending interneurons (Song et al., 1997).

However, there were some differences in the active electrophysiological characteristics of viscerofugal neurons between the present study in organ cultured tissue and the previous study in an acute preparation. Sharkey et al (1998) reported that all colonic viscerofugal neurons either fired a few action potentials at the onset of depolarizing current pulses or were inexcitable (mean number of action potentials to depolarization 1.5 ± 2). Furthermore they reported that about 25% received spontaneous synaptic inputs. In contrast, in the present study many viscerofugal neurons fired repetitively throughout depolarizing current pulses (1-25 action potentials, mean 6.4 ± 7.7, 21 cells, n=12) and about 85% received spontaneous fast synaptic inputs. It is possible that the process of organotypic culture contributed to these differences. Organ culture might artefactually increase the excitability of enteric neurons. Alternatively, the period of several days in culture may allow preparations to recover from the acute trauma caused by dissection. In addition, discrepancies may arise from different populations of neurons being sampled. In the present study, viscerofugal neurons were filled from colonic nerves entering the specimen of gut and may innervate any of the prevertebral ganglia (Kuramoto and Furness, 1989, Furness et al., 1990c, Messenger and Furness, 1992, 1993) or the pelvic plexus (Luckensmeyer and Keast, 1995a). In contrast, Sharkey et al labelled only neurons which projected to the inferior mesenteric ganglion. In the present study, 72% of viscerofugal neurons were immunoreactive for nitric oxide synthase, whereas only 8% contained NOS immunoreactivity in the previous study (Sharkey et al), suggesting that different populations may have been sampled.

Most viscerofugal neurons in the present study (>85%) received frequent spontaneous fast excitatory synaptic inputs compared to about one quarter in the previous study. One possible cause of this difference is a fine detail of the dissection. In the present study, care was taken to avoid damage of the myenteric plexus; often a thin layer of circular muscle remained attached to myenteric ganglia (see **figure 6.22** and **6.23**). In addition, strips of intact circular muscle were left at either end of the preparation to facilitate pinning. It has been reported that some mechanosensory S-neurons in the myenteric plexus of guinea pig colon have processes in superficial circular muscle and may actually require some of the circular muscle to generate stretch-evoked action potentials (Spencer and Smith, 2004, Spencer et al., 2006). We speculate that more thorough removal of circular muscle in the present study may have reduced spontaneous firing activity in preparations.

Nicotinic fast synaptic inputs unequivocally contribute to the excitation of viscerofugal neurons. However, it is possible that viscerofugal neurons also receive non-nicotinic fast synaptic inputs. Purinergic and serotonergic fast synaptic events have been shown in colonic neurons (LePard et al., 1997, Nurgali et al., 2003a). In the present study, nicotinic receptor blockade was tested on a single viscerofugal neuron, blocking all spontaneous fast synaptic input to that neuron, and was shown to abolish all electrically-stimulated fast synaptic input in a single viscerofugal neuron recorded by Sharkey et al. (1998). These are small samples and the possibility remains open that non-nicotinic inputs may contribute to fast synaptic excitation of viscerofugal neurons.

*Subpopulations of viscerofugal neurons*

Most previous studies have reported that viscerofugal neurons have single axons and Dogiel type I or "simple" cell morphology (Kuramoto and Furness, 1989, Furness et al., 1990c, Messenger and Furness, 1992, 1993, Anderson et al., 1995, Sharkey et al., 1998, Tassicker et al., 1999a, Lomax et al., 2000, Olsson et al., 2004, Hibberd et al., 2012c, b). In accumulated studies of several hundred viscerofugal neurons in the distal colon, well labelled by biotinamide, we found rare instances of multipolar viscerofugal neurons with Dogiel type II neuron morphology (accounting for fewer than 1%). The single multipolar viscerofugal neuron impaled in the present study had typical "AH" neuron characteristics that have been described in Dogiel type II neurons. This neuron had a pronounced shoulder on the repolarization phase of action potentials, a "sag" in membrane potential to membrane hyperpolarisation (reflecting an $I_H$ current), and a long after-hyperpolarization following a single action potential. This neuron also lacked both spontaneous and electrically-stimulated fast EPSPs and did not respond to direct application of 10μM DMPP. This is consistent with the low level of expression of nicotinic receptors reported for this type of neuron previously (Ermilov et al., 2003).

The present study suggests that uni-axonal viscerofugal neurons may comprise 2 subtypes, differentiated by their immunoreactivity to NOS. Nitric oxide is a putative neuromodulator in prevertebral sympathetic ganglia (Szurszewski and Miller, 2006), expressed in populations of viscerofugal neurons (Furness and Anderson, 1993, Anderson et al., 1995, Mann et al., 1995, Olsson et al., 2004), and also supplied by spinal sensory neurons (Zheng et al., 1997b) as well as sympathetic preganglionic neurons (Furness and Anderson, 1993, Anderson et al., 1995). Nitric oxide exerts

dual inhibitory and excitatory effects in guinea pig and mouse prevertebral neurons (Mazet et al., 1996, Browning et al., 1998). To date there is no direct evidence linking nitrergic neurotransmission in sympathetic ganglia to viscerofugal neurons. However, nitric oxide from viscerofugal neuron inputs may underlie slow hyperpolarizations evoked by colonic distension in the inferior mesenteric ganglia (Hankins and Dray, 1988). In the celiac ganglia, NOS-immunoreactive terminals of colonic viscerofugal neurons preferentially target secretomotor sympathetic neurons, suggesting a role in modulating intestinal secretion (Costa and Furness, 1984, Anderson et al., 1995). However, whether viscerofugal nerve terminals that lack NOS immunoreactivity show a similar selectivity, remains to be determined. In the present study, NOS-immunoreactive viscerofugal neurons were larger and more dendritically complex than viscerofugal neurons that lacked NOS. They also tended to have more positive resting potentials and receive more synaptic inputs than their NOS-lacking counterparts. Put together, these findings suggest that there may be 2 subtypes of viscerofugal neurons, but this possibility requires further study for confirmation.

All viscerofugal neurons that were recorded electrophysiologically in the present study contained detectable ChAT immunoreactivity (11 cells, n=4). Of a total of 120 DiI-labelled viscerofugal neurons that were not electrophysiologically recorded, 105 (87.5%) contained detectable ChAT immunoreactivity. This suggests that a small population of viscerofugal neurons may not use acetylcholine. To date, no studies have measured the proportion of viscerofugal neurons that use acetylcholine as a transmitter. All viscerofugal neurons with projections to the coeliac or inferior mesenteric ganglion contained ChAT immunoreactivity (Mann et al., 1995, Sharkey

et al., 1998). Therefore the 15 DiI-labelled viscerofugal nerve cell bodies that lacked detectable ChAT immunoreactivity may have projections to other targets via colonic nerve trunks, including the superior mesenteric ganglion (Messenger and Furness, 1993), major pelvic ganglia (Luckensmeyer and Keast, 1995a), or spinal cord (Doerffler-Melly and Neuhuber, 1988, Suckow and Caudle, 2008).

In conclusion, targeted intracellular recordings from retrogradely labelled viscerofugal neurons were made in guinea pig colon. Electrophysiologically, all but one viscerofugal neuron had properties consistent with myenteric S-neurons. Selective pharmacological activation of functional synaptic inputs to viscerofugal neurons showed that they receive numerous inputs from locally projecting neurons in nearby myenteric ganglia. The synaptic inputs to viscerofugal neurons evoked from oral myenteric ganglia were stronger than inputs evoked from aboral ganglia.